FACULTE DES SCIENCES
Département de Chimie

Centre for Education and Research on Macromolecules – Prof. Christine Jérôme

Development of non-isocyanate polyurethane-based hydrogels as drug-eluting implants

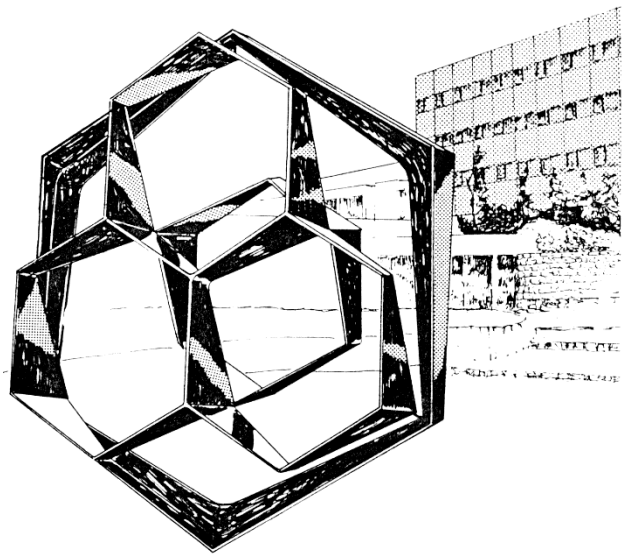

Année académique 2023-2024

Dissertation présentée par
Antoine Delvaux
en vue de l'obtention du diplôme de
Master en Sciences Chimiques

Remerciements

Ce travail représente non seulement pour moi l'aboutissement du Master en Sciences Chimiques, mais également l'accomplissement d'un objectif personnel lié à un parcours académique qui a pris quelques détours à son commencement, avant de finalement trouver sa voie. Ceci n'aurait pas été possible sans un certain nombre de personnes, je souhaitais donc profiter de ces quelques lignes pour les remercier de leur aide précieuse.

Je voudrais tout d'abord remercier le Prof. Christine Jérôme pour m'avoir donné l'opportunité de réaliser mon mémoire dans son laboratoire. L'année écoulée fut très enrichissante autant au niveau de l'apprentissage qu'au niveau personnel et je lui en suis très reconnaissant.

Je tenais à remercier l'ensemble des membres de mon comité de lecture, le Prof. Christine Jérôme, le Dr. Raphaël Riva, le Dr. Bruno Grignard et le Prof. Anna Lechanteur pour avoir accepté de faire partie de mon jury.

Je souhaiterais également remercier le Dr. Raphaël Riva, pour sa disponibilité constante tout au long de ce mémoire et pour tout le temps qu'il a consacré à la relecture de ce travail. Je le remercie également pour la confiance qu'il m'a accordée lors de ce travail de recherche.

Je tenais à remercier Mme Martine Dejeneffe, qui m'a grandement aidé pour mes manipulations et sur qui je pouvais toujours compter en cas de soucis. Je la remercie également particulièrement pour sa patience et son aide lors de mes premiers jours au sein du laboratoire.

Je souhaiterais remercier l'ensemble des membres du CERM pour leur accueil chaleureux et pour la bonne ambiance générale qui règne au laboratoire.

Je voulais également remercier mes amis proches qui m'ont soutenu lors des périodes plus difficiles de mes études.

Pour terminer, je tenais à remercier ma famille avec qui j'ai pu traverser les mauvais moments et partager les bons. Je remercie Éric pour ses conseils, grâce auxquels je me suis orienté vers le CERM pour mon mémoire. Je remercie mes parents pour m'avoir toujours soutenu et pour m'avoir permis de réaliser ce parcours.

Table of contents

List of abbreviations

CuI	Copper iodide
CO_2	Carbon dioxide
UV	Ultraviolet
PEO	Polyethylene oxide
PPG	Polypropylene glycol
PU	Polyurethane
NIPU	Non-isocyanate polyurethane
HU	Hydroxyurethane
REACh	Registration, Evaluation, Authorisation and Restriction of Chemicals
NMR	Nuclear magnetic resonance
HPLC	High performance liquid chromatography
DSC	Differential scanning chromatography
T_g	Glass transition temperature
TBAOPh	Tetrabutylammonium phenolate
DMF	Dimethylformamide
DMSO	Dimethyl sulfoxide
DCM	Dichloromethane
TMS	Tetramethyl siloxane
DBU	1,8-Diazabicyclo(5.4.0)undec-7-ene
BisCC	Bis-cyclic carbonate
AAS	Acetylsalicylic acid

Introduction

Abstract

This work aims at reporting on the development of a new formulation route for a drug-eluting vaginal hydrogel implant. At this moment in time, the considered implant present on the marketplace is produced according to a strategy based on the reaction of polyols with diisocyanate, a hazardous reactant whose use is increasingly subject to strict regulation. This work targets the development of an isocyanate-free alternative formulation strategy based on the substitution of diisocyanate by a bis-cyclic carbonate which is a CO_2-sourced molecule less dangerous to use. The main goals of this research will be to define the experimental conditions required to produce the bis-cyclic carbonate-based implant compatible with an application as drug eluting medical device and to determine the impact of the formulation on the physico-chemical properties and on the release profile of a model encapsulated drug.

Dans ce travail, nous rapportons les avancées sur le développement d'une nouvelle voie de formulation d'un implant vaginal en hydrogel pour la libération de principe actif. Actuellement, l'implant dont il est question est synthétisé suivant une stratégie basée sur la réaction de polyols avec un di-isocyanate, un réactif dangereux qui est sujet à un nombre croissant de nouvelles régulations. Ce travail se concentre sur le développement d'une voie de formulation alternative, sans isocyanates, basée sur la substitution du di-isocyanate par un di-carbonate cyclique, une molécule CO_2 sourcée moins dangereuse à employer. Les objectifs principaux de ce travail seront la détermination des conditions expérimentales optimales pour la production des implants à base de di-carbonates cycliques compatibles avec leur emploi en tant que dispositifs médicaux pour la libération de principe actif, ainsi que la détermination de l'impact de cette formulation sur les propriétés physico-chimiques de l'implant et sur le profil de relargage d'un principe actif modèle imprégné dans l'implant.

Context of the research

When a medication is prescribed to a patient, the critical question is to define the optimal method of administration and the perfect dosage to have the suitable therapeutic effect without unwanted side-effects. Moreover, in too many cases, a lessening of the drug activity occurs by premature elimination and/or degradation of the drug, typically by the hepatic clearance or renal filtration. Localized administration represents an efficient answer to circumvent these limitations, as it drastically reduces both the distance and the residence time required for the drug to reach the targeted site. Creams or viscous gels are perfect examples of local drug administration presenting the advantage of being easy to apply to any shape but suffering from a lack in stability over time, which is problematic for storage considerations [1].

A viable alternative lies in drug-eluting implants, which are able to release the active principle (API) in a controlled manner, which can be determined either by their physical structure and/or their chemical composition. They can be implanted directly into tissues via a surgical procedure, which is still an invasive administration method that can cause discomfort and pain to the patient. However, in some favourable cases such as vaginal implants for women's health, the implantation site is easily accessible without requiring surgery [2–4].

Drug-eluting implants

Drug-eluting implants are already largely present on the marketplace and allow for the administration of many drugs in specific pharmaceutical applications. For example, Gliadel® is a monolithic degradable polymer implant used in brain cancer therapy [5]. Jadelle® is a contraceptive implant classified as a reservoir implant, which consists in a drug-loaded core surrounded by a polymer membrane through which the drug diffuses. Other types of drug-eluting implants include stents, which are rigid tubular structures inserted into the vessel lumen to avoid obstruction. However, such implants bear the intrinsic risk of causing post-intervention complications. To address this issue, drug-loaded stents have been experimented with, and it has been shown that this solution decreases the rate of complication events from 20-30% down to 3-20% [2,6,7].

As shown by the previous examples, the applications for drug-eluting implants are numerous and varied. Such variety requires adaptable materials in order to perfectly fit to the targeted application, which makes polymer materials ideal candidates. However, it is important to keep in mind that the implantation site is the human body. Thus, precautions must be taken to ensure that no deleterious side-effects will affect the host. The selected polymers must thus be biocompatible, defined as the ability of a material to perform with an appropriate host response when applied as intended [8]. If the implant is degradable, it is also crucial that the degradation products are biocompatible and non-toxic. They must either be metabolized or easily eliminated by the organism. Another important point is the purification process of the implant. If dangerous components, such as heavy metals for example, are used during the synthesis step, they must be correctly eliminated from the implant before implantation into the patient. The release kinetics of the loaded drug is also of importance, as a badly designed implant could cause a burst effect, which could be harmful depending on the nature of the loaded active principle.

One of the main goals of drug-eluting implants, compared to classical drug absorption (daily medication (pills), repeated intravenous injections, …), is to improve the patient compliance and the therapeutic efficiency [1]. In this way, their shapes are precisely designed to perfectly fit to the administration site. The release of the drug is assured either through a diffusion or a degradation mechanism. In the first case, the implant releases the drug without being distorted while in the second case, the degradation of the implant leads to the release of the drug in the environment [9,10].

Diffusion-controlled elution

The main mechanism of the drug release out of a hydrogel is based on a diffusion process. The driving force for this phenomenon is the gradient of concentration existing between the implant (high drug concentration) and the external environment, poor in drug [2,9,10]. Depending on the design of the implant, the diffusion rate can be controlled. If the implant is composed of a matrix in which the drug is uniformly dispersed, the diffusion rate is proportional to the square root of time at the early state of the elution [6]. In the case of a more complex system consisting in the combination of a core reservoir containing the drug and a surrounding polymer shell, the diffusion rate of the active principle is kept constant and thus, does not depend on the time [11,12]. Those mechanisms are represented in the Figure 01, as well as their corresponding drug-release profile.

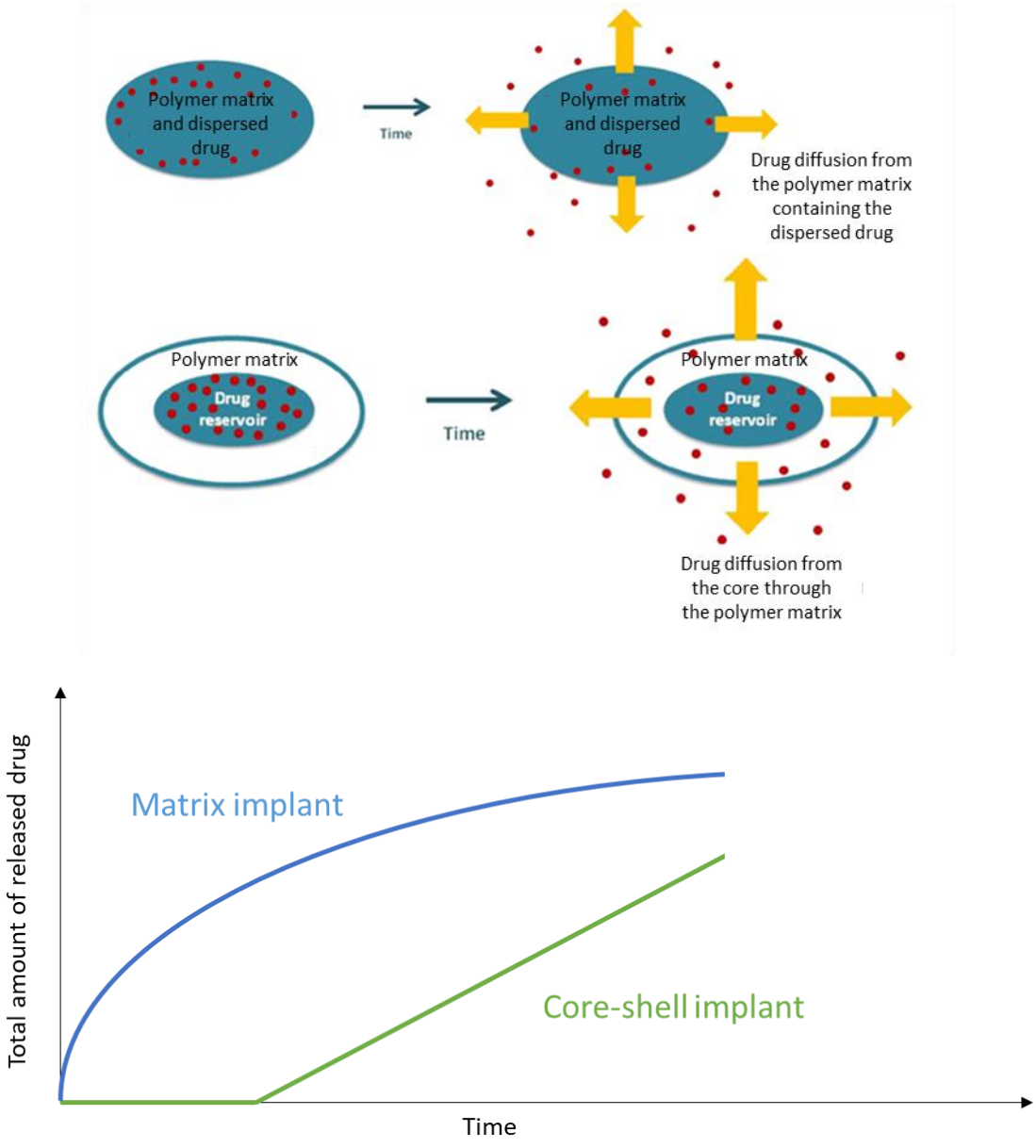

Fig. 01: Schematic representation of the drug release by diffusion for simple drug-loaded matrix and core-shell hydrogel implant [6]

Degradation-controlled drug release

In the case of drug loaded implants made of a degradable polymer, the release can be both due to diffusion and the slow degradation of the implant itself. After implantation at the targeted site, the biological environment causes the degradation of the polymer chains, with formation of oligomers, allowing the drug to be released into the organism. The kinetics of release is controlled by the degradation rate of the polymer. For this strategy, it is also highly important that the degradation products do not provoke harmful effects to the surrounding tissues and are easily eliminated by the organism [5,10,11]. The Figure 02 illustrates the degradation phenomenon and the associated drug-release profile[12].

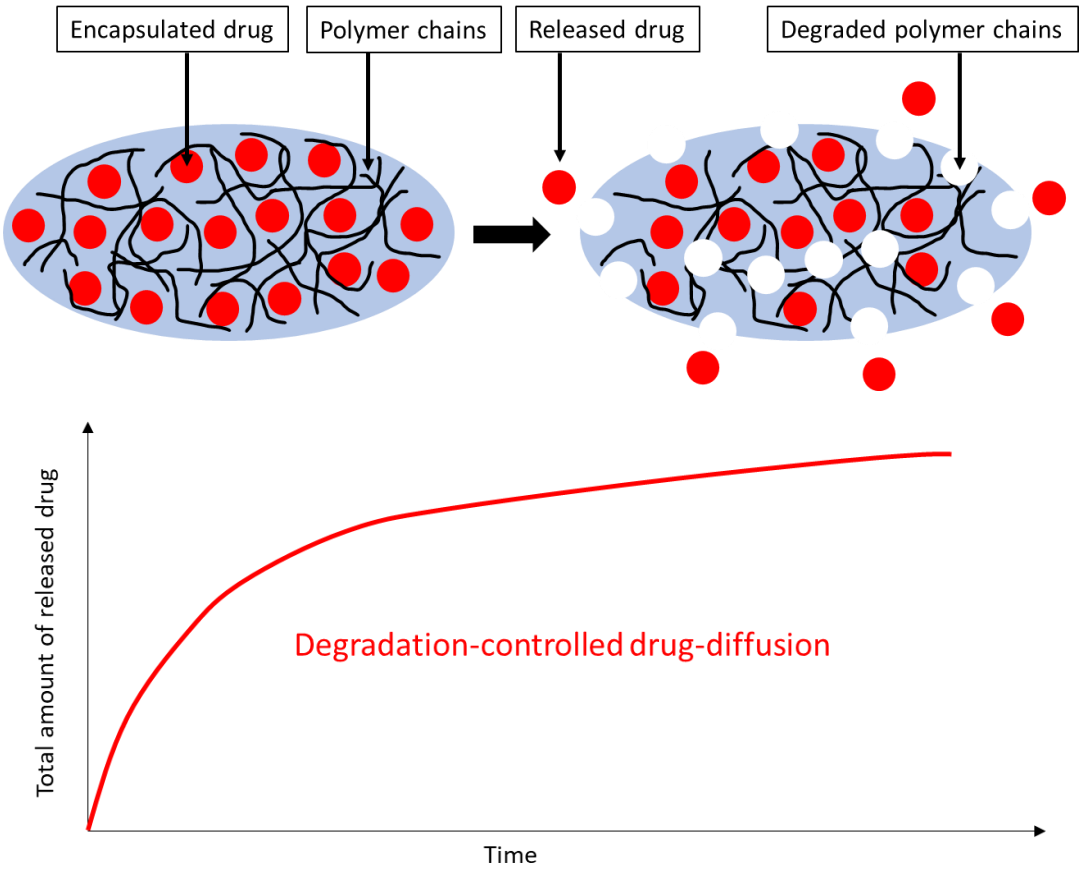

Fig. 02: Schematic representation of drug release by degradation of the polymer matrix

Polymer hydrogels

A hydrogel is a three-dimensional network of a hydrophilic polymer which is largely swollen in water[6,13,14]. Gels are mainly made up of liquids, namely water in case of hydrogels, but have a behaviour close to that of solids thanks to their three-dimensional network physically or chemically crosslinked within the liquid. The high-water content of a hydrogel provides physical properties similar to those of human tissues, which enhances the

biocompatibility of the implant and allows for the efficient encapsulation of hydrophilic drugs [14]. Moreover, the diffusion of the encapsulated drug out of the hydrogel is driven by the crosslinking density of the hydrophilic polymer, which can be easily customized to perfectly fit to the required drug-release profile.[15].

Crosslinked polymers can be obtained through two main routes, namely physical or chemical crosslinking. In the first case, the chains entanglement and/or weak interactions between specific groups present on the polymer chains are responsible of the network formation, making them reprocessable. Those interactions may be hydrogen bonding [16], ionic interaction [17], Van der Waals interactions [18,19] or phase separation in the case of block copolymers [20]. At the opposite, the different polymer chains of chemically crosslinked polymers are linked by covalent bonds leading to highly stable networks [13]. Chemical crosslinking can be achieved following different strategies, such as the copolymerization of a monomer with a difunctional agent, the photo-crosslinking under UV irradiation [21–23], the vulcanization [24] or the reaction of homotelechelic polymer chain-ends with a polyfunctional reactant. In this last example, the network's mesh-size might be better controlled by the crosslinking density which depends on the molar mass of the linear chains and the amount and functionality of the polyfunctional reactant (crosslinker). It has a deep impact on the drug diffusion and mechanical properties of the material. Indeed, hydrogels with a higher crosslinking rate are characterized by higher mechanical resistance as the network is stiffer and exhibits lower swelling rates [25].

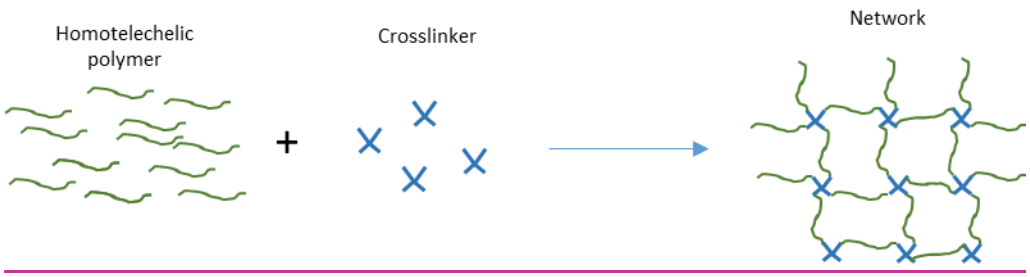

Fig. 03: Chemical crosslinking of linear polymer chains with a trifunctional crosslinker

Swelling

When a crosslinked polymer is immerged in a solvent for which it has an affinity, it will swell due to the absorption of the solvent into the meshes of the network, leading to a gel. Indeed, the solvent and the polymer chains of the network will interact together leading to the solvation of the latter. However, as the polymer chains are linked together by the crosslinking nodes, no dissolution occurs but rather swelling of the material. The equilibrium degree of swelling can be determined using the following equation:

$$Q = \frac{V_{Swollen}}{V_{Dry}} = \frac{V_P + V_S}{V_P} = \frac{1}{\phi_P}$$

Where:

- Q is the equilibrium degree of swelling
- $V_{Swollen}$ is the volume of the fully swollen gel
- V_{Dry} is the volume of the dried gel
- V_P is the volume of the polymer
- V_S is the volume of the solvent
- Φ_P is the volume fraction of the polymer

The swelling phenomenon can be described by the monitoring of the variation of the mixing free-enthalpy ($\overline{\Delta G_{mix}}$) and of the free-enthalpy of deformation ($\overline{\Delta G_{Elas}}$). The former characterizes the interactions between the polymer and the solvent, while the latter is linked to the stretching of the polymer network. Indeed, the more the polymer swells to absorb more solvent, the harder it is for the chains to move relatively from one another as the tension in the network increases. The swelling phenomenon is represented in the Figure 04.

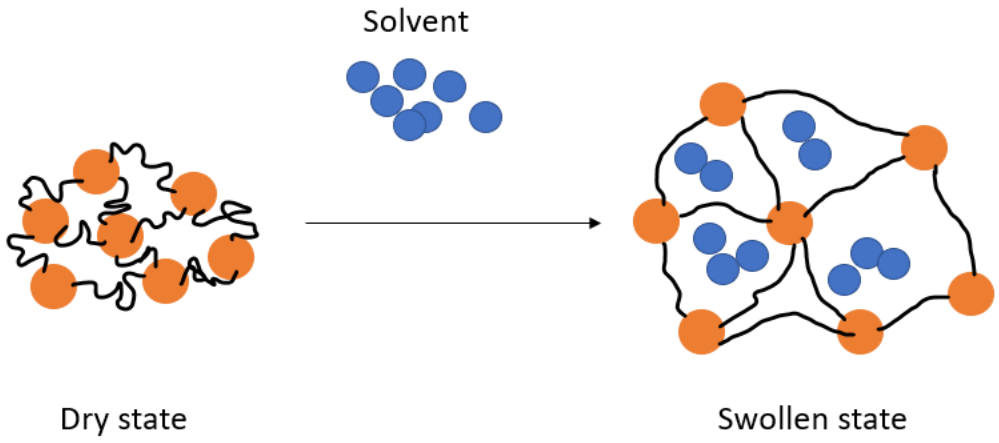

Fig. 04: Swelling phenomenon

For the polymer to be able to swell, $\overline{\Delta G_{mix}}$ must be negative, this value can be calculated using the Flory-Huggins theory. This gives us the following equation:

$$\overline{\Delta G_{mix}} = RT\left[\chi {\phi_P}^2 + \ln(1-\phi_P) + \phi_P\right]$$

Where:

- R is the gas constant
- T is the temperature
- χ is the Flory-Huggins parameter

In this equation, the Flory-Huggins parameter can be accessed experimentally. Indeed, the formula of the osmotic pressure is as follows:

$$\Pi = \frac{\phi}{N} - \ln(1-\phi) - \phi - \chi\phi^2$$

Where:

- Φ is the volume fraction of monomer
- N is the number of monomers in the polymer
- Π is the osmotic pressure

Using this equation, it is possible to compute the value of the χ parameter by conducting multiple measures of the osmotic pressure for the considered mix of polymer and solvent.

To determine the limit of the swelling, it is also necessary to consider $\overline{\Delta G_{Elas}}$, which can be calculated by the Flory-Rehner theory, using the following equation (affine model):

$$\overline{\Delta G_{Elas}} = RT\frac{\rho_P V_S}{M_C}{\phi_P}^{1/3}$$

Where:

- ρ_P is the density of the polymer
- M_C is the average molar mass of a chain between two crosslinking nodes

For the network to swell, the sum of those two free-enthalpies has to be negative thus, following this theory, the swelling carries on up until $\overline{\Delta G_{Tot}} = 0$, which can be translated to $\overline{\Delta G_{mix}} = -\overline{\Delta G_{Elas}}$ as $\overline{\Delta G_{Tot}} = \overline{\Delta G_{mix}} + \overline{\Delta G_{Elas}}$, giving us one last equation:

$$\chi {\phi_P}^2 + \ln(1-\phi_P) + \phi_P = -\frac{\rho_P V_S}{M_C}{\phi_P}^{1/3}$$

Drug impregnation in crosslinked material

The swelling of a crosslinked material is a crucial parameter in the context of this research, both for the loading of the active principle according to an impregnation process and for its release afterwards. The drug loading occurs by immersion of the dry implant into a solution containing a determined quantity of active principle. The selected solvent must be a good solvent of both partners, allowing the active principle to penetrate deeply in the network as the steric hindrance is lessened by the swelling of the polymer chains. After reaching the maximum of swelling, the solvent is then removed under vacuum with a shrinking of the material, effectively trapping the active principle in the mesh of the network [11,13,14,26].

Drug release out of crosslinked material

As detailed earlier, the elution of the drug out of the implant can take place either via degradation of the polymer network or via diffusion. In the scope of the present work, we focus on the diffusion mechanism, as it is the one considered for the implant developed during this project.

The release of a drug out of a crosslinked material consists simply in the migration of the active principle through the meshes of the network. If the hydrodynamic volume of the drug is smaller than the mesh size of an available neighbouring space in the network, the molecules can migrate to this new position. The nature of the solvent also affects the efficiency of the phenomenon. Indeed, if the solvent is favourable for the API, it will ease its diffusion out of the matrix. Another variation of this release mechanism is to control the kinetics via gel swelling. After implantation in the body, the hydrophilic network swells with the biological fluids. This swelling induces the stretching of the polymer chains in the network, allowing for the encapsulated drug to breach the barrier initially caused by the steric hindrance. The molar flux of the drug is then described as [6,14]:

$$J = -D * \Delta c$$

Where:

- J is the molar flux of the drug
- D is the diffusion coefficient in the polymer
- Δc is the difference in drug concentration between the polymer and the exterior

Considering the time variable, we can access the kinetics of the drug release:

$$\frac{\partial c}{\partial t} = -\Delta J = \Delta(D * \Delta c)$$

The crosslinking rate of the implant also has an significant influence on the kinetics of elution, as the drug has to travel through the polymer network to reach the exterior environment. If the network's mesh-size is high (e.g. polymer chains with high molar mass are present between two crosslinking nodes), it is easier for the drug to move inside the network and thus the diffusion rate is faster than in the case of network presenting small mesh-size, i.e. for densely crosslinked networks [6]. The affinity of the drug for the polymer also plays a crucial role in the mechanism. Better is the affinity between the active principle and the polymer constituting the network, longer will be the time required for the drug to be released. By playing on both crosslinking density and the nature of the polymer constituting the network, an adapted release profile for a specific drug can be reached.

Polyurethane-based hydrogels

Isocyanate route

Many hydrogels are currently used as drug-eluting implants, generally obtained by the crosslinking of hydrophilic polymer chains, mainly biocompatible polyethylene oxide (PEO). Different crosslinking strategies are reported in the literature[6]. Among them, the reaction of an isocyanate with the hydroxyl chain-ends of PEO was successfully used in the case of Cervidil®, a commercially available intravaginal implant.

Typically, commercially available α,ω-dihydroxyl PEO was reacted with a diisocyanate to get a polyurethane in presence of a triol molecule acting as crosslinking agent [27]. The polyurethane network is then formed based on hydrophilic PEO chains linked to the crosslinking nodes by urethane links (Fig. 05).

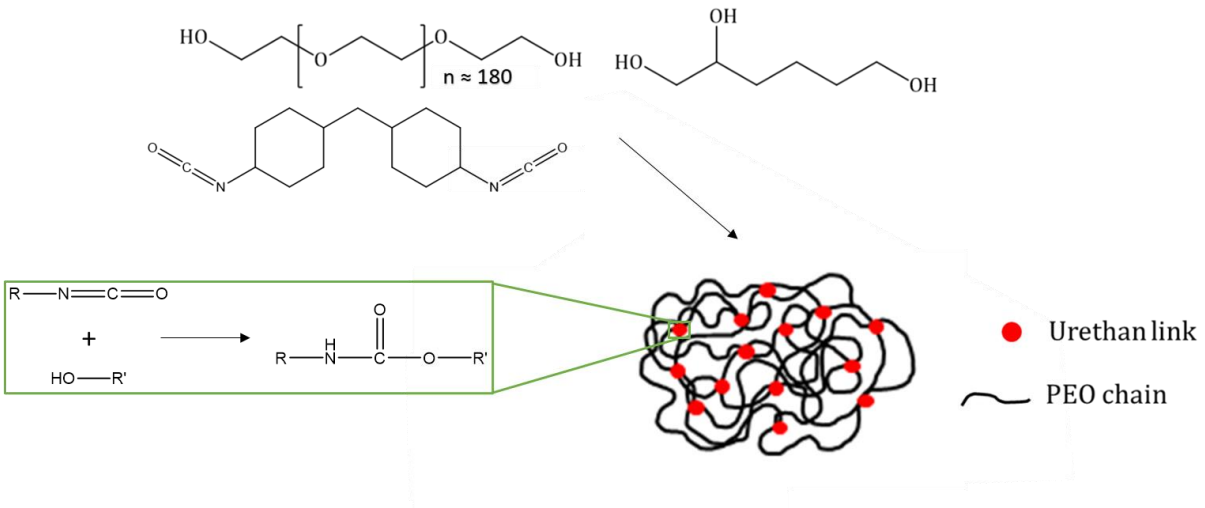

Fig. 05: Schematic representation of components for Cervidil® implant formulation

The formation of urethane moieties using isocyanate is a well-known and common reaction in the industry. Indeed, polyurethanes are used in a large range of applications, such

as coating, foams, or gels. This versatile reaction is not restricted by precise conditions and can occur at ambient temperature, which is the case for the foaming process [28,29].

However, the isocyanates are strong irritant reactants that can cause serious health issues if handled without adapted precautions. Moreover, some isocyanates are highly flammable and explosive, which can lead to higher risks of accident during handling. The synthesis of those components is also an issue as isocyanates are the product of the phosgenisation of amines:

$$RNH_2 + COCl_2 \rightarrow RNCO + 2\,HCl$$

The storage of isocyanates also requires special attention as they react easily with water to produce carbon dioxide:

$$RNCO + H_2O \rightarrow RNH_2 + CO_2$$

For those reasons, the REACh committee decided on February 4, 2020, on the interdiction of di-isocyanates as reactants for the 24 August 2023 [30–32].

Cyclic carbonate as alternative of isocyanate

This new regulation forced the industries to invest in the development of alternative routes for the synthesis of polyurethane-based materials. A new family of polymer, non-isocyanate polyurethane (NIPU) has emerged from this need to develop alternative ways for polyurethane synthesis.

The urethane function is accessible through various reactions, such as the rearrangement of an acyl azide or the ring-opening polymerization of a cyclic carbamate [32]. However, all those alternatives use toxic reactants and, for some, phosgene derivatives, which is still an issue regarding the safety of the process.

A safer route was however found in the reaction of amines with cyclic carbonates [33]. This reaction has the advantage of not using any isocyanates or phosgene derivatives. Indeed, cyclic carbonate are synthesised by different routes such as the addition of carbon dioxide into an epoxide [34] as illustrated in the Figure 06.

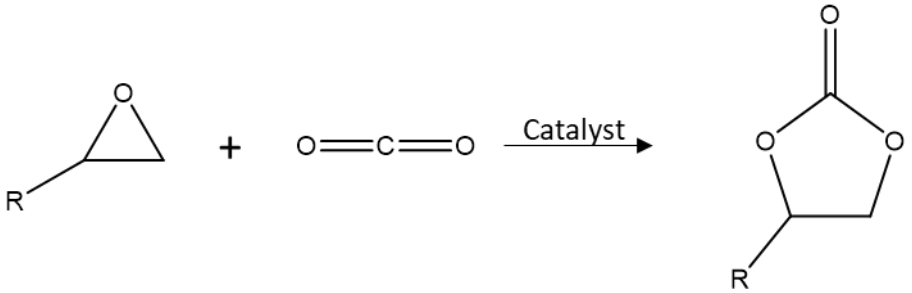

Fig. 06: Carbonatation of an epoxide into a cyclic carbonate

Moreover, the storage of the cyclic carbonates does not require any particular cautions as they are weakly reactive, non-toxic and not sensitive to hydrolysis [35]. As illustrated in Figure 08, the ring-opening of cyclic carbonate by a primary amine does not release any side products. However, the resulting product is not exactly a urethane as it presents a pendant hydroxy group. It has therefore been named hydroxyurethane (HU) (Figure 07).

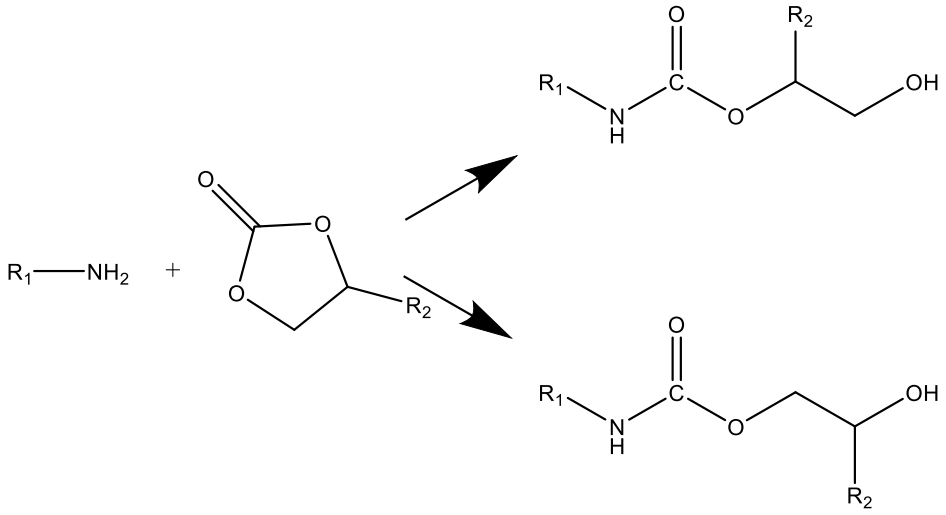

Fig. 07: Formation of hydroxyurethanes by ring-opening reaction of a cyclic carbonate by a primary amine.

The presence of this pendant hydroxy group changes the interactions between the molecules themselves and between the molecules and the environment. Moreover, this reaction is characterized by the formation of two distinct products depending on the bond broken during the cycle opening [33].

For highly specific applications, the presence of two products may be a limitation. In order to overcome this issue, the use of unsaturated cyclic carbonates is a convenient approach [36]. Indeed, the presence of a conjugated unsaturation activates the ring-opening in a specified direction, assuring the reproducibility of the collected product. Moreover, as a five-member ring, the cyclic carbonate is a stable and low reacting cyclic molecule, which could lead to longer reaction times and/or harsher temperature conditions in order to reach high yields. Other activating groups may be grafted into the cyclic carbonate to increase its reactivity, it is thus possible to obtain propylene carbonate methacrylates[37] or glycerine carbonate vinyl ether[38] for example. In the case of this work, we focus on the vinyl group as the substituent on the cycle, which improves the reaction between the cyclic carbonate and the amine. This reaction is illustrated in the Figure 08.

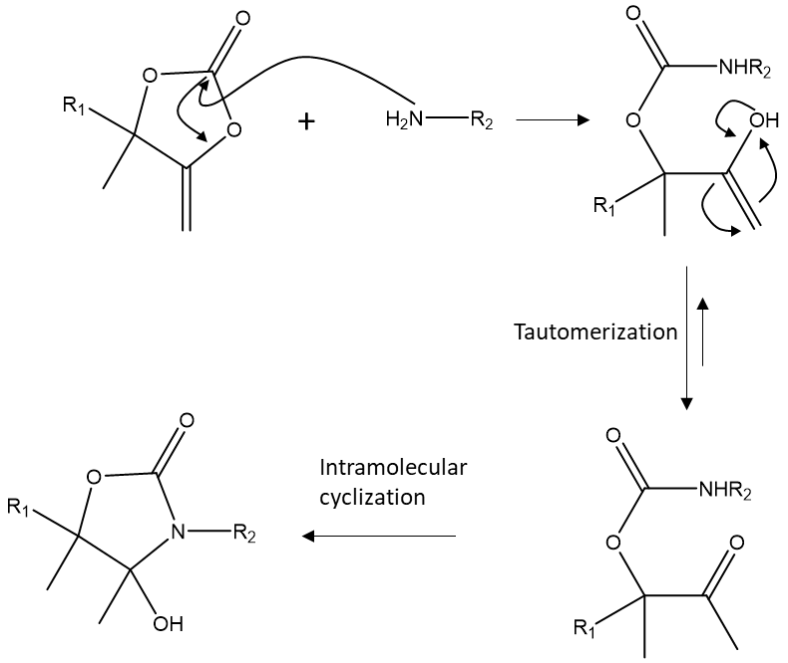

Fig. 08: Formation of the oxazolidone function

Similarly, to the conventional cyclic carbonates, the exo-vinylene cyclic carbonates are synthesised using carbon dioxide as a reactant. Indeed, they are accessible through the addition of CO_2 on a propargylic alcohol, as illustrated by the Figure 09.

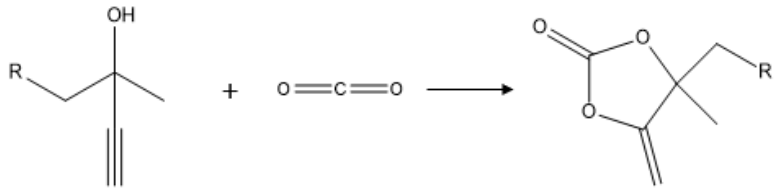

Fig. 90: Synthesis of an exovinylene cyclic carbonate

With the purpose to apply the ring-opening reaction of exo-vinylene cyclic carbonates by an amine for polymer synthesis, bis-cyclic unsaturated carbonates were successfully synthesised and reacted with diamines leading to non-isocyanate polyurethane via step-growth polymerization according to a polyaddition reaction (Figure 10) [36].

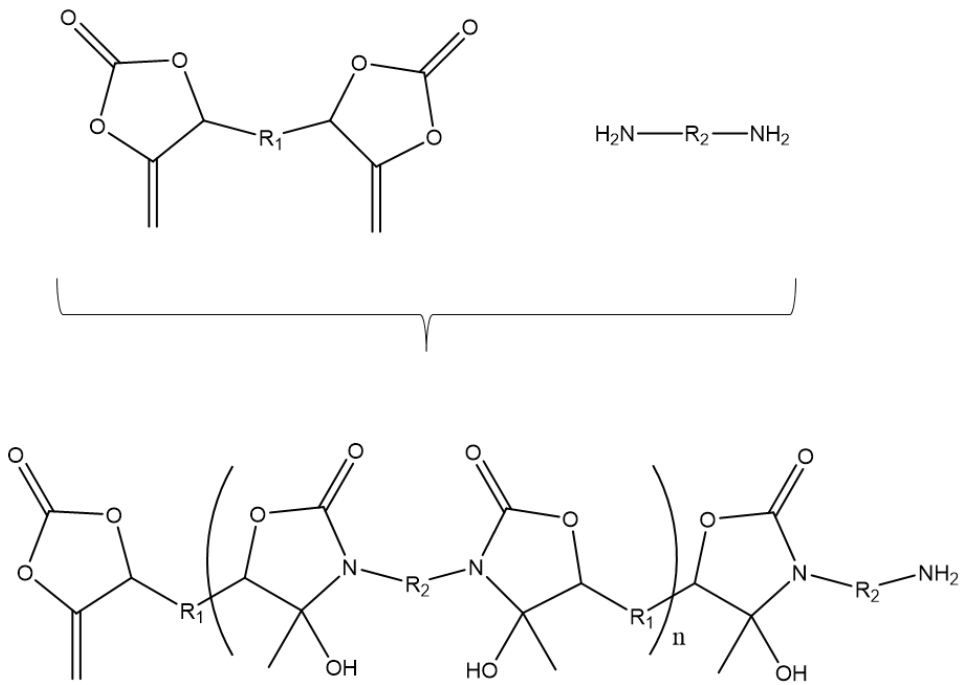

Fig. 10: Synthesis of NIPUs via polyaddition of unsaturated bis-cyclic carbonates and diamines

Objective and strategy

The main challenge of this work is to define the experimental conditions necessary to synthesise an isocyanate-free polyurethane drug-eluting hydrogel implant based on PEO. According to literature, unsaturated cyclic carbonates are selected to reach this goal. We aim to study the impact of the hydrogel composition on the mechanical properties and the ability to release in a controlled manner an active principle.

For this purpose, the reaction between commercially available hydrophilic Jeffamine® (α,ω-diamine poly(propylene oxide)-*b*-PEO-*b*-poly(propylene oxide) triblock copolymer) and bis-cyclic carbonates bearing an exocyclic unsaturation in the presence of a polyamine crosslinker is investigated, leading to formulation of crosslinked hydrophilic material.

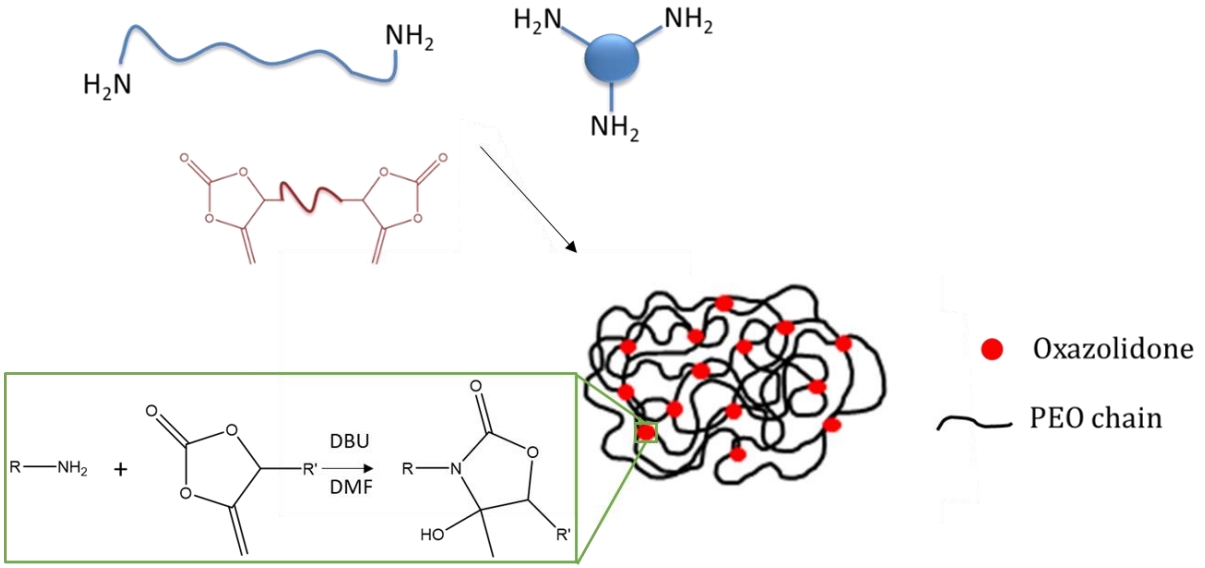

Fig. 11: Network formation by reacting PEO amine chain-ends with bis exo-vinylene cyclic carbonates in presence of triamine compound.

The implant will thus be composed of a chemically crosslinked polymer formed of hydrophilic polyethylene glycol segments linked together by the oxazolidone functions.

The network crosslinking density will be assured by the addition in the reactive mix of the tri-amine compound (crosslinking agent) while the size of the network mesh will be controlled by the molecular weight of the linear Jeffamine®. The weight ratio between the Jeffamine® and the crosslinking agent in the reactive mix allows us to adapt the permeability of the network after swelling in water, key parameter to allow for the controlled release of a loaded active principle, but also the mechanical properties of the hydrogel.

This work is divided into two main goals. The first one is the formulation of a NIPU implant using a bis-cyclic carbonate linked via an ethyl chain (called here “linear bis-cyclic carbonate") (Fig 12 A) synthesised in the laboratory, a commercially available Jeffamine® ED2003® (MW = 1900 g/mol) (Fig 12 G), and a commercially available tri-amine compound, the tris(2-aminoethyl)amine (TREN) (Fig 12 D). The formulation conditions for this implant will be optimized and a complete characterization will be carried out.

In a second time, alternative bis-cyclic carbonates (Fig 12 B and C) and tri-amines (Fig 12 E and F) will be introduced to determine their impact on the properties of the implant. These different implants will then be compared to the isocyanate-based one to identify the most pertinent candidate for its replacement.

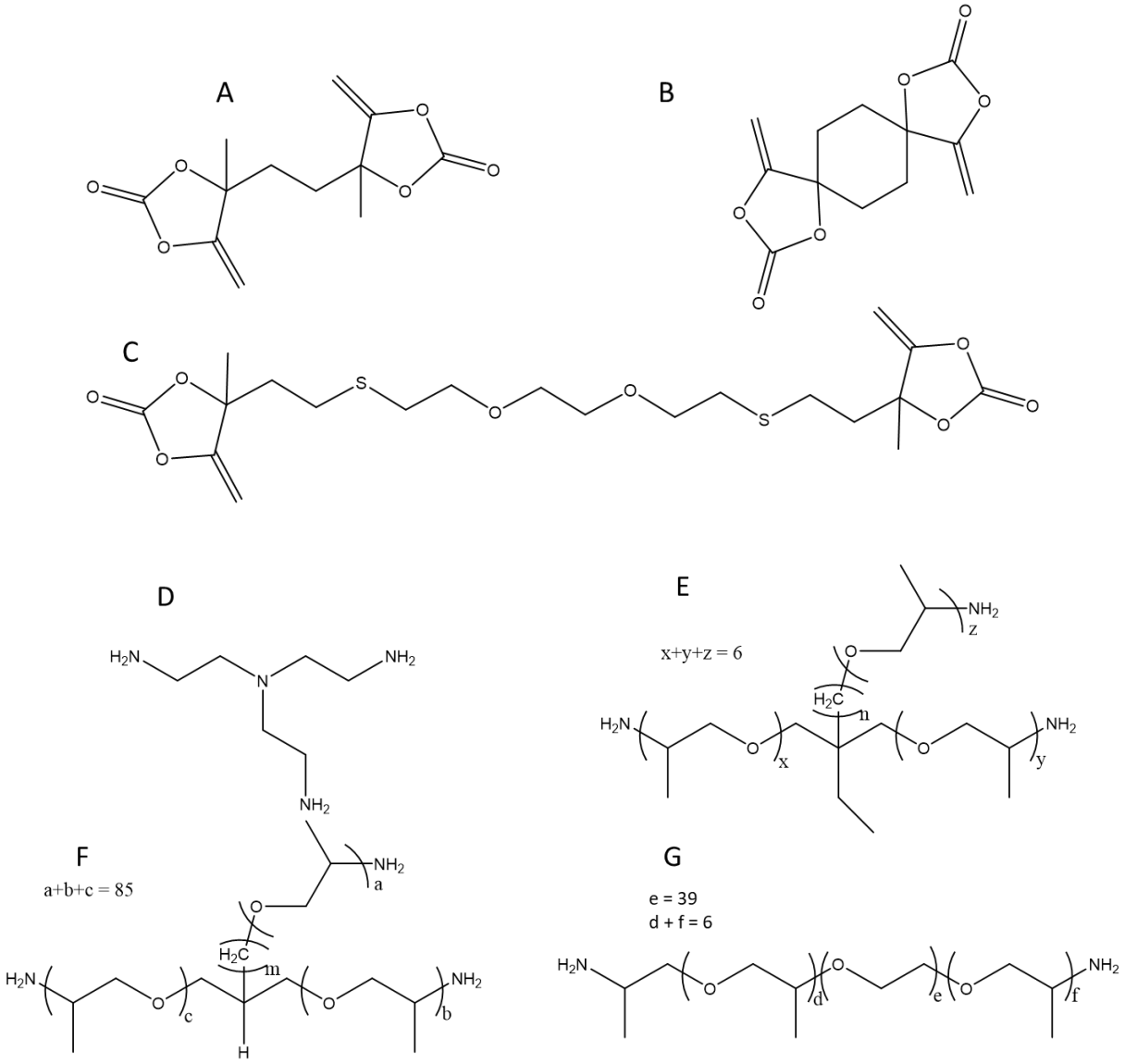

Fig. 12: List of the bis-cyclic carbonates, the di-amine and the tri-amines used during this research: A = Linear bis-cyclic carbonate; B = Cyclic bis-cyclic carbonate; C = Liquid bis-cyclic carbonate; D = TREN; E = Jeffamine® T403 (MW = 440 g/mol); F = Jeffamine® T5000 (MW = 5000 g/mol); G = Jeffamine® ED2003 (MW = 1900 g/mol)

In order to determine precisely the impact of each modification of the reactive mix on the network properties, only one parameter at a time will be changed between two different formulations (nature of the crosslinking agent, nature of the bis-cyclic carbonate, solvent, …). Once the different series of implant are formulated, a thorough comparison will be conducted between them (swelling ratio, insoluble fraction, glass transition temperature, mechanical properties, …). The impact of each modification will help us to define the key parameters to formulate an implant presenting the physico-chemical characteristics in agreement with the specifications defined starting from the commercially available isocyanate-based implant.

Finally, the ability of the obtained networks to load a model active principle by an impregnation process and to release it in a controlled manner will be determined according to usual pharmaceutical release tests. After determination of the release profile, adjustments could be carried out on the composition of the reactive mix with the aim to approach even more the characteristics imposed by the specifications.

Results and discussion

The research is divided into three main parts. In the first one, we investigated the impact of the structure of the unsaturated bis-cyclic carbonate used for the formulation of the NIPU implant on drug loading and release properties in comparison with classical isocyanate PU. The spacer between the cyclic carbonate functions was either an ethyl or a cyclohexyl group. Then, the nature of the crosslinker was investigated while keeping constant the other components of the NIPU formulation. Unsaturated bis-cyclic carbonate linked by an ethyl chain was used for this study. Finally, an unprecedented bis-cyclic carbonate that is liquid at room temperature was synthesised and tested for the synthesis of NIPU networks by a solvent-free process.

Investigation on the impact of the structure of the bis-cyclic carbonate

This first part focuses on the use of both the linear and cyclic bis-cyclic carbonates for the formulation of the NIPU implants. These bis-cyclic carbonates were selected as a starting point for the experiments as their synthesis was already optimized thanks to previous research in the laboratory. The choice was also motivated by the hypothesis that the modification in the nature of the bis-cyclic carbonate's spacer (from an ethyl to a cyclohexyl one) would have some impact on the properties of the final network.

Synthesis of the linear bis-cyclic carbonate

Briefly, ethynylmagnesium bromide was added on the starting hexane-2,5-dione to produce a bis-propargylic alcohol (3,6-dimethylocta-1,7-diyne-3,6-diol). After purification, carbon dioxide was added on the alcohol using tailored catalysts under supercritical CO_2 conditions. The overall process is illustrated in the Figure 13.

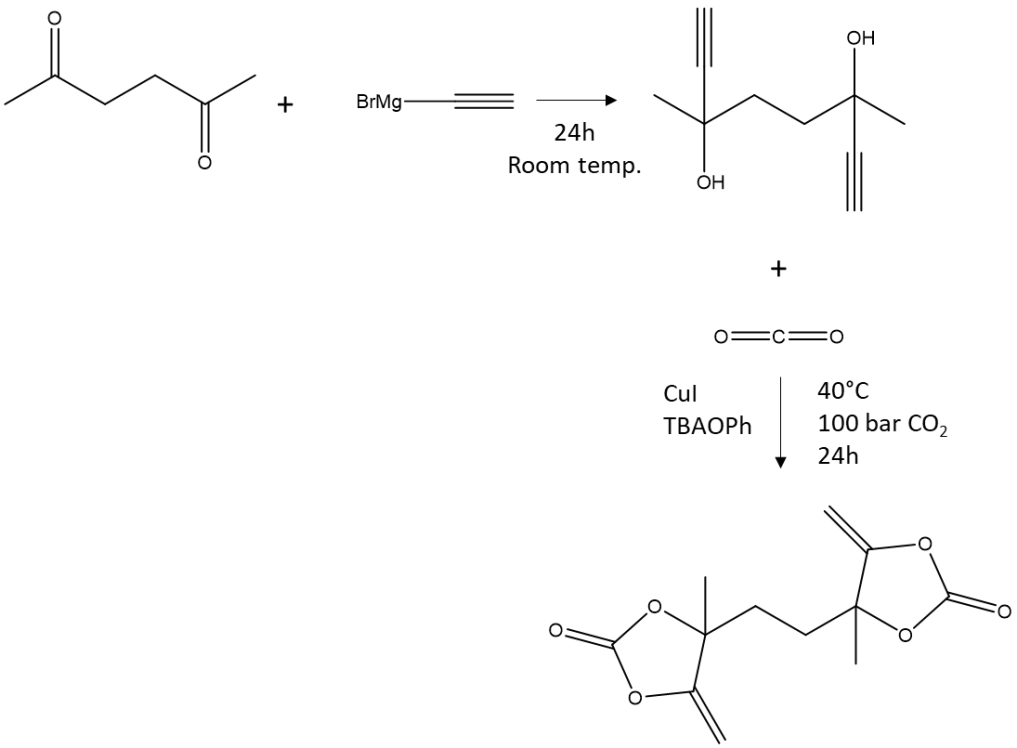

Fig 13: Synthesis strategy for the linear bis-cyclic carbonate

After purification of the product, the bis-cyclic carbonate was dried and kept in a desiccator in order to avoid hydrolysis.

The structure of the "linear bis-cyclic carbonate" was assessed by proton nuclear magnetic resonance spectroscopy, using dimethyl sulfoxide-d_6 as solvent. The spectrum is presented in the Figure 14.

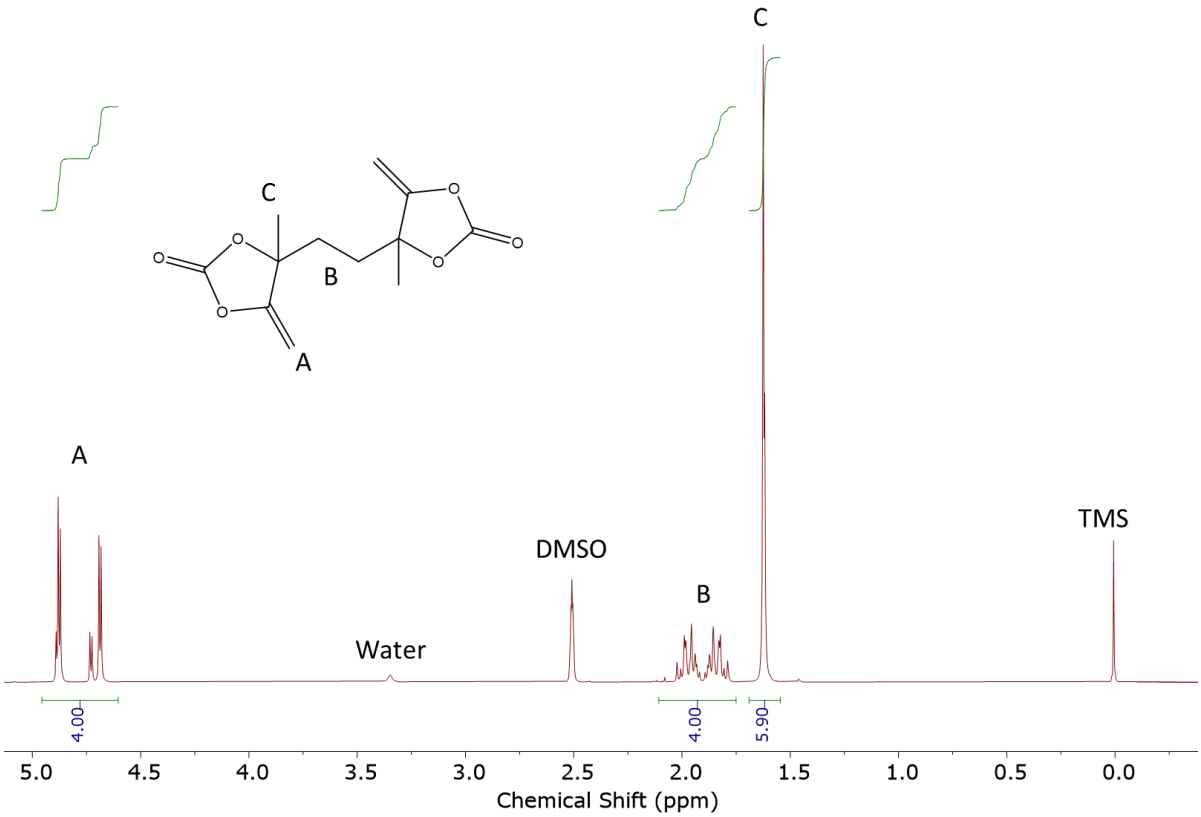

Fig. 14: ^{1}H NMR spectrum of the linear bis-cyclic carbonate

The remaining peaks on the spectrum correspond either to the solvent (DMSO, peak at 2.54 ppm) or the water it contains (peak at 3.33 ppm), the product was thus deemed pure enough for us to use.

Nevertheless, even with a storage under inert atmosphere, the bis-cyclic carbonate is partially degraded with time. A possible explanation is the reaction of the cyclic carbonate with water, causing an opening of the rings and a release of carbon dioxide, effectively deactivating the reactant for the reaction with the amines. Even with the careful storage conditions we established, it was necessary to occasionally recrystallize the compound.

Synthesis of the cyclic bis-cyclic carbonate

The synthesis of this second bis-cyclic carbonate follows the same strategy as for the linear bis-cyclic carbonate. The only difference is the starting diketone, which changes to the cyclohexane-1,4-dione. Briefly, ethynylmagnesium bromide was added on the starting diketone to produce a propargylic alcohol (1,4-diethynylcyclohexane-1,4-diol). After purification, carbon dioxide was added on the alcohol using tailored catalysts under supercritical CO_2 conditions. As for the linear bis-cyclic carbonate, the structure was assessed by proton nuclear magnetic resonance spectroscopy, using dimethyl sulfoxide-d_6 as solvent. The spectrum is presented in the Figure 15.

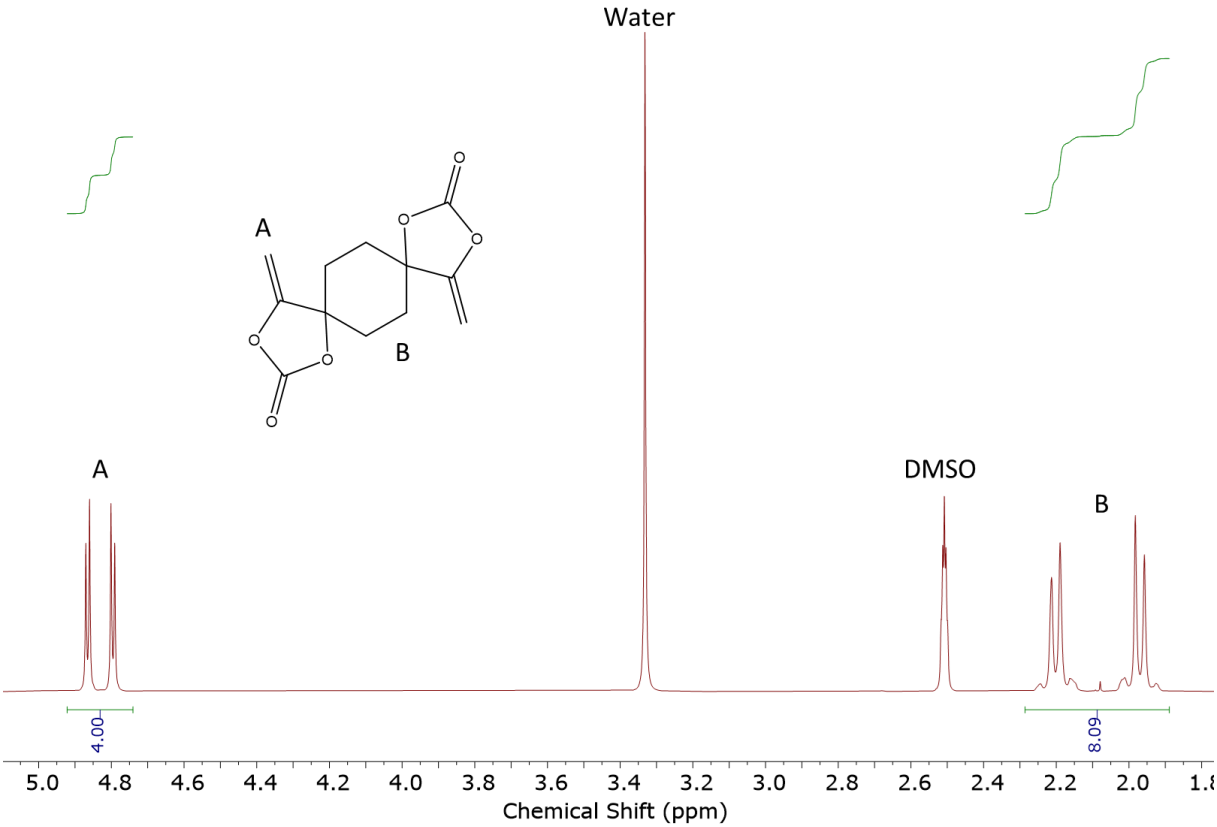

Fig. 15: NMR ^{1}H spectrum of the cyclic bis-cyclic carbonate

The remaining peaks are attributed either to the solvent used for the analysis (the peak of the DMSO is situated at 2.54 ppm) and to the water contained in the solvent (peak at 3.33 ppm).

Design of the typical bis-cyclic carbonate route

After the successful synthesis of the linear bis-cyclic carbonate, the next goal of this research was to set up a formulation protocol allowing for the synthesis of NIPU-based hydrogel implants. Indeed, the protocol used for the synthesis of isocyanate-based hydrogel implant cannot be directly applied for the preparation of NIPU-based hydrogel implants. The isocyanate-based implant was produced by mixing hexanetriol (crosslinking agent) with a α,ω-dihydroxyl polyethylene oxide (PEO-diOH, MW = 8000 g/mol) in presence of dibutyltin dilaurate as catalyst at the molten state. Liquid 4,4'-dicyclohexyl diisocyanate was then added to the mix under stirring to initiate the crosslinking. The solution was then quickly poured into molds and pressed to produce plates from which the implants can be cut at the desired shape. In the case of NIPU-based implants, the reaction rate between cyclic carbonate and hydroxyl group was very slow. Moreover, the melting point of the linear bis-cyclic carbonate is very high (148°C), and it degrades rapidly at the molten state. The consequence of these two observations was that we could not simply replace the liquid diisocyanate by the solid bis-cyclic carbonate that is insoluble in the molten PEO.

In order to allow for the formulation of NIPU-based hydrogel implants, we substituted PEO-diOH by commercially available Jeffamine® ED 2003. This polymer is a triblock copolymer made of a central block of PEO and two lateral blocks of poly(propylene oxide) characterized by the presence of primary amine groups at both chain-ends, which are more reactive than hydroxyl groups towards cyclic carbonate. In the same way, hexanetriol must also be replaced by a triamine compounds to get an urethane group and the tris[2-(dimethylamino)ethyl]amine (TREN) was selected. With the purpose to reach a liquid formulation, allowing the injection in a mold, the addition of dimethylformamide (DMF), a solvent known to effectively solubilize the linear bis-cyclic carbonate, was investigated. The quantity of each reactant was chosen in order to obtain a stochiometric mix in regard of the number of functions, this assured an equal amount of amine and cyclic-carbonate functions. Those quantities are included the Table 01.

Composition of the NIPU implant				
	Linear bis-cyclic carbonate	Jeffamine® ED2003	TREN	DBU
m (g)	0.5828	1.1168	0.1662	0.0200
n (mol)	0.0023	0.0006	0.0011	0.0001
n functions (mol)	0.0046	0.0012	0.0034	0.0001

Table 01: Composition of the linear bis-cyclic carbonate-based implant

The strategy for the formulation of the NIPU implant, based on the inherent restrictions of the used reactants, is detailed in the Figure 16.

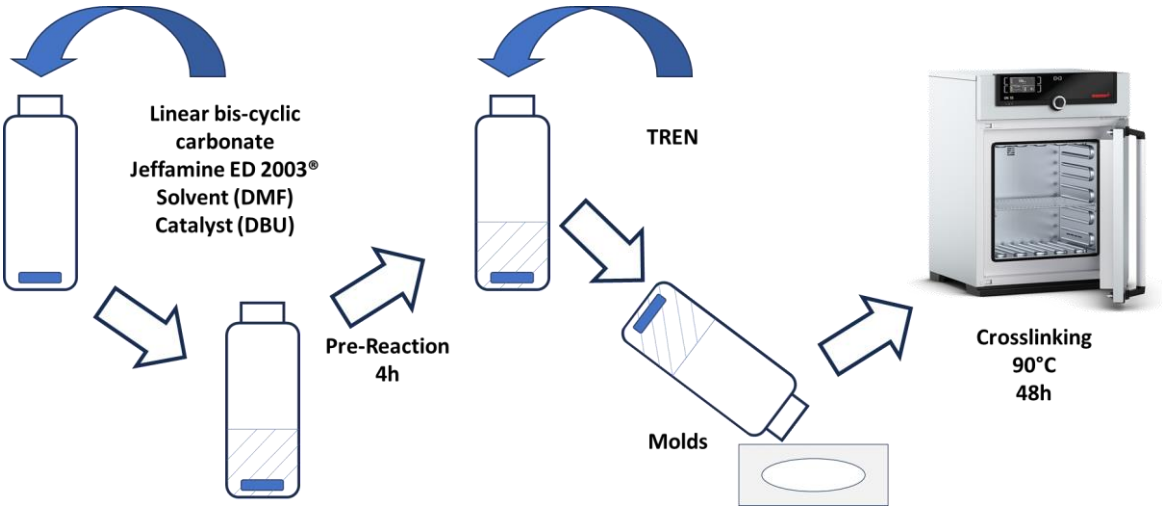

Figure 16: Formulation process of the NIPU implant

Typically, the NIPU networks were produced by solubilizing Jeffamine® ED2003 and the linear bis-cyclic carbonate in anhydrous DMF (2 ml) in presence of DBU as catalyst. The solution was stirred under inert atmosphere for 4 hours before adding the TREN to initiate the crosslinking. This 4-hour period of pre-reaction was required because the amine chain-ends of Jeffamine® ED2003 are less reactive than the amine groups of TREN, which led to a faster reaction between the bis-cyclic carbonate and the crosslinking agent with formation of non-

homogenously crosslinked implant. The pre-reaction allowed for the quantitative conversion of the amine chain-ends of Jeffamine® into cyclic carbonate chain-ends able to react with the crosslinker. The solution was then poured into molds which were kept in an oven for 2 days. After 2 days of crosslinking in a specific mold designed to directly confer the targeted shape during which the majority of DMF was evaporated, solid implants were successfully recovered, as shown in the Figure 17.

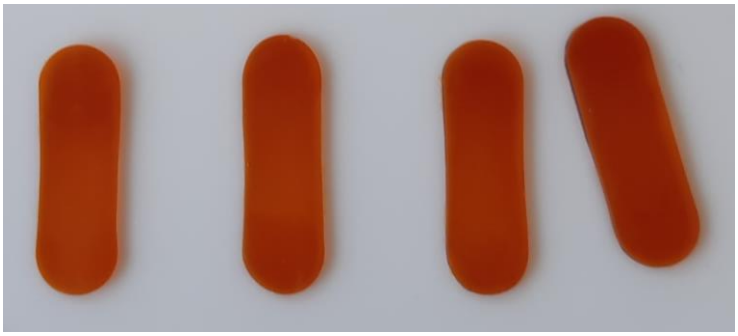

Fig. 17: NIPU implants

For the formulation based on the use of the cyclic bis-cyclic carbonate, the overall strategy was the same as for the linear one. However, it was observed that the solubility of the cyclic bis-cyclic carbonate in DMF was lesser than for the linear one. The formulation process had to be adapted to take this limitation into account. The volume of DMF was kept equal but the quantity of all the reactants was halved. This allowed for the solubilisation of all the compounds while keeping the stoichiometry of the solution. Those quantities are included in the Table 02.

Composition of the NIPU implant				
	Cyclic bis-cyclic carbonate	Jeffamine® ED2003	TREN	DBU
m (g)	0.2891	0.5584	0.0831	0.0100
n (mol)	0.0011	0.0003	0.0006	0.0001
n functions (mol)	0.0023	0.0006	0.0017	0.0001

Table 02: Composition of the cyclic bis-cyclic carbonate-based implant

Swelling rates

In order to confirm the efficiency of the crosslinking reaction, the swelling rate of the collected implants was measured after 24 hours of immersion in water, i.e. a good solvent of the polymer precursor. A kinetics analysis of the evolution of the swelling rate in water was conducted, which confirmed that the maximum of swelling was reached after 24 hours. The crosslinking efficiency in function of the duration of the crosslinking step was then followed. In addition, we also tested the impact of a drying step of the linear bis-cyclic carbonate prior to the crosslinking reaction. The results are represented in the Figure 18.

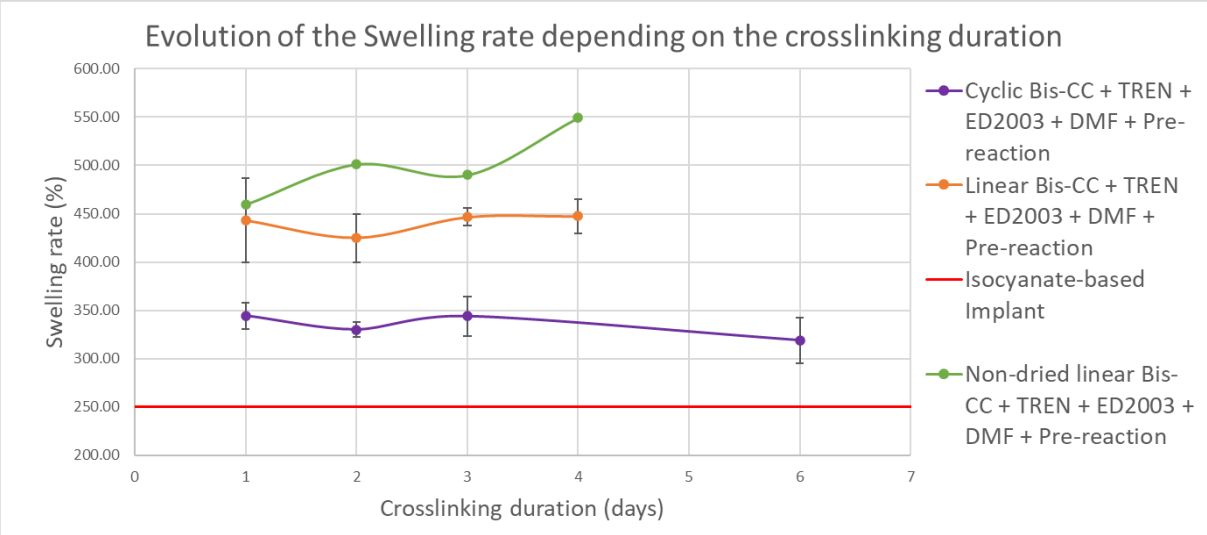

Fig. 18: Swelling rates in water in function of crosslinking reaction time for different implants made of linear bis cyclic carbonate/Jeffamine® ED2003/DMF and TREN with drying step (orange curve) or without drying step (green curve) and cyclic bis-cyclic carbonate/Jeffamine® ED2003/DMF and TREN (violet curve) compared to the isocyanate-based implant (red curve)

The results showed that the swelling rate of the linear bis-cyclic carbonate-based network was stable in time after 1 day of curing in the oven (447.35 % ± 17.96%) but was much higher than the swelling rate of the isocyanate-based one (250%). A discrepancy was to be expected as the structure of the network was thoroughly modified. This difference is lessened for the cyclic bis-cyclic carbonate-based implant, which can be explained qualitatively by the Flory-Rehner theory. As the network was stiffer than the previous one, it required more energy to absorb more solvent and to keep swelling. The modification of the spacer could also have an impact on the Flory-Huggins parameter, thus changing the behaviour of the hydrogel. Moreover, the transition from a linear to a cyclic spacer diminish the hydrophilicity of the network, which also explains the value of the swelling rate (318.88% ± 23.42%).

While the networks were in all cases synthesised from stochiometric mixtures regarding the number of functional groups, the length of the chains between two crosslinking nodes was significantly greater in the isocyanate-based implant. However, this modification alone should have decreased the swelling rate of the implant, given the Flory-Rhener theory. The soluble fractions were calculated to assess the efficacity of the crosslinking step and find

an explanation for these results. It was found that 20% of the total mass was lost during the first swelling of the linear bis-cyclic carbonate-based implant against 9% for the cyclic bis-cyclic carbonate-based one and 13% for the isocyanate one. As these values do not significantly differ, the explanation for the results of the swelling rate experiment must lie elsewhere. It is possible that the crosslinking step was not as efficient for the NIPU implants. As the results indicated, 1 to 2 days are required to obtain a stable swelling rate, meaning that the kinetics of the reaction is much slower than in the case of the isocyanate-based implant. It is thus possible that the crosslinking agent had not entirely reacted with the cyclic carbonate functions, leaving more pending chains than in the case of the isocyanate-based implant and thus increasing the theoretical swelling rate. Another explanation could lie in the probable partially physical crosslinking of the isocyanate implant. Indeed, as the PEO chains are longer than for the NIPU implant, it is conceivable that those chains are physically entangled in the network, increasing the stress applied by the swelling and thus limiting this phenomenon. Unfortunately, those last two hypotheses were not explored in the scope of this Master thesis.

The results also show that the water has an impact on the crosslinking rate of the implant. Indeed, the Figure 18 shows that the swelling rate of the implant made from the non-dried reactants (green curve) is higher than the swelling rate of its dried counterpart (orange curve). The non-dried implant was able to swell further because the water present in the solution during the formulation deactivated part of the cyclic carbonate functions, effectively lowering the crosslinking rate. This resulted in a looser network, which could then reach higher swelling rates as explained by the Flory-Rehner theory. Therefore, to get a better reproducibility of the network, dried bis-cyclic carbonate will be used systematically for the formulations.

Thermal properties of the networks

Differential scanning calorimetry (DSC) measurements were conducted to determine the crystallinity rate of the implant as well as their glass transition temperature (T_g). The crystallinity rate may have an impact on the swelling kinetics of the implant as the crystalline structures have to dissolve for the implant to fully swell. The measurement of the glass transition temperature helps determine the state in which the implant will be used. The results are illustrated in the Figures 19 and 20.

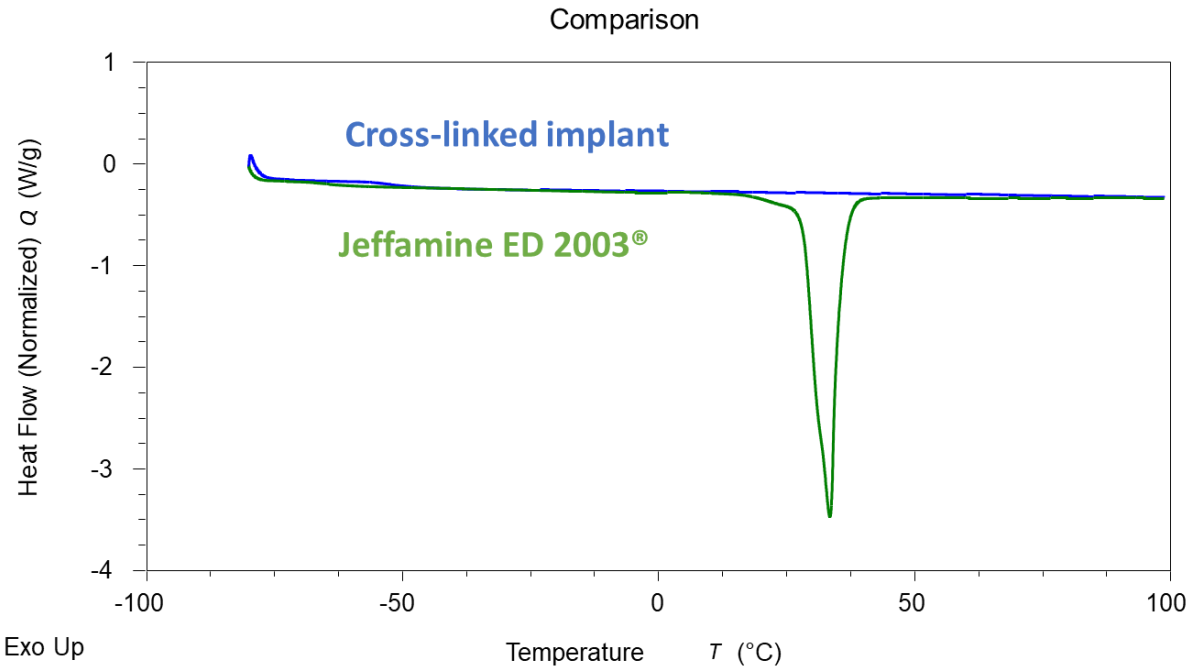

Fig. 19: Comparison of the DSC curves (second scan) between the starting Jeffamine® ED 2003 (green) and the cured linear bis-cyclic carbonate/ED2003/DMF/ TREN formulation (blue)

This analysis highlighted the presence of a crystallinity peak in the DSC graph of the Jeffamine® ED2003, while none were observable in the case of the cross-linked NIPU implant. The disappearance of the crystallinity of the crosslinked Jeffamine® is an indication of the success of the crosslinking. The reduced mobility of the crosslinked chains prevents their organisation in crystallites upon cooling.

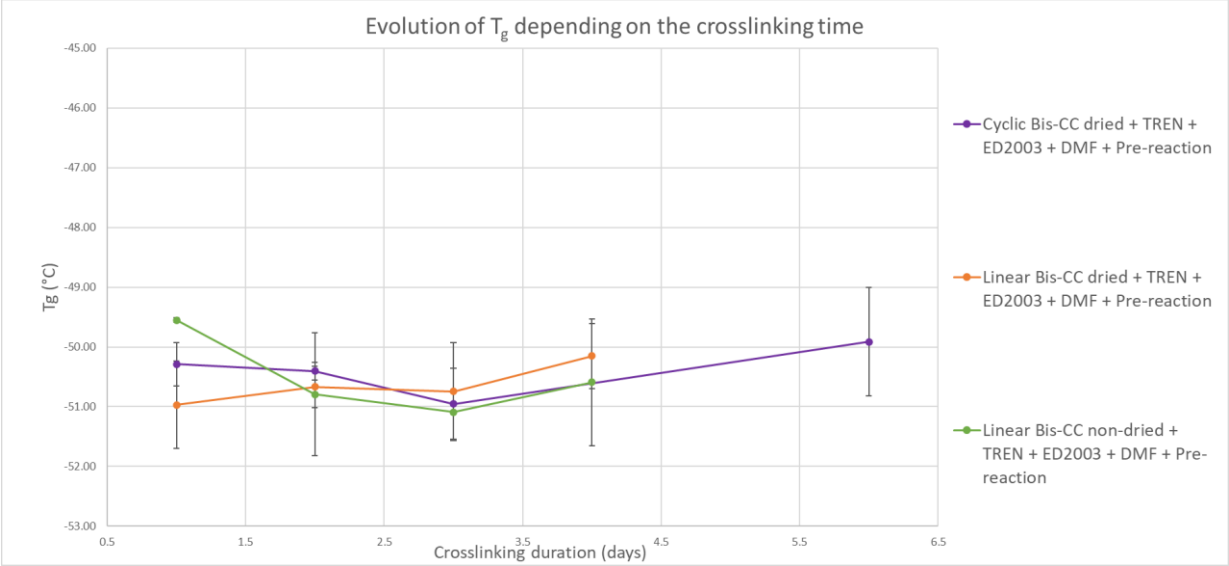

Fig. 20: Comparison of the T_G of the different implant formulations: dried (orange curve) and non-dried (green curve) linear bis-cyclic carbonate and cyclic bis-cyclic carbonate (violet curve)

Here, the impact of the crosslinking duration on the glass transition temperature of the implant was monitored by DSC. Similarly to the measurements of the swelling rates, the results indicated that the T_g is more time-dependant for non-dried bis-cyclic carbonate-based

formulations (Fig 20. green curve), showing the importance of drying for the sake of reproducibility.

The results also illustrated the impact of the crosslinking on the glass transition temperature of the polymer. Indeed, Jeffamine® ED 2003 has a T_g of -63.78°C while the T_g of the crosslinked implants lies around -50°C. The formation of the urethane functions thus impacts the glass transition of the polymer by increasing it. The melting temperature of the diamine also disappears as the crosslinking prevents the network from crystallizing.

Finally, as illustrated by the Figure 20, the modification of the bis-cyclic carbonate had no significant impact on the glass transition temperature of the implant which remains dominated by the Jeffamine® (the mass of the bis-cyclic carbonate only represents 51% of the mass of the Jeffamine®).

Drug loading

The study of the drug-loading and drug-release properties of the implant were conducted using acetylsalicylic acid as a model molecule. This choice was motivated by the wide availability of this drug, as well as its relatively low cost. Moreover, this API did not require specific handling caution. The quantification by high performance liquid chromatography (HPLC) method was also well-defined in the laboratory.

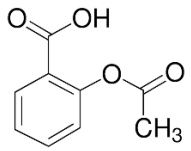

Fig. 21: chemical structure of the acetylsalicylic acid

Briefly, in order to load the implants with acetylsalicylic acid, the NIPU networks at the dried state were impregnated by immersion for two hours in a solution of the API in dichloromethane (DCM) at a concentration of 0.2 g/L. A prior swelling rate kinetics analysis was conducted to determine the required immersion time. It was concluded that the implant reached its maximum swelling rate after 1 hour. It was thus decided to let the implant for 2 hours in the impregnation solution to ensure an efficient loading step. The loaded implants were then dried and kept in a desiccator until the analysis of the drug-release profile. The drug loading was impossible to determine by HPLC method since the implants are made of insoluble crosslinked materials. It is thus impossible to isolate the drug effectively loaded by solubilisation of the matrix of the implant. Moreover, because of the presence of DMF trapped in the networks due to the formulation process, it was not possible to determine the loading rate by gravimetry. Thus, it was decided to define the drug loading of the implants as the final ceiling value of the release rate profile based on the approximation that 100% of the loaded drug was released at the end of the process.

DCM was chosen as the solvent for the impregnation step as it is a good solvent for both the drug and the polymer chains of the implant. This allowed for a rapid impregnation as

well as a fast-drying step as the DCM is a very volatile solvent. The loading conditions were kept unchanged throughout the loading of each series of implant in this work. The swelling rates of the linear bis-cyclic carbonate implant, the cyclic bis-cyclic carbonate one and the isocyanate-based one were respectively 967.84%, 2278.85% and 801.47% in DCM. The higher value obtained for the NIPU network seems to confirm the lower efficiency of the crosslinking in this case as compared to the PU. Nevertheless, the difference is much lower than in water which might reflects the increased hydrophilicity of the NIPU as compared to PU, notably due to the hydroxy group on the oxazolidone.

Drug-release profile

HPLC analysis was used to determine the drug-release profile of the implants. Typically, dry AAS-loaded NIPU implants (79.6 mg for the linear bis-cyclic carbonate based one and 22.7 mg for the cyclic bis-cyclic carbonate based one) were each immerged in 2 ml of water, the vial was then placed in an incubator at 37°C to start the release of the drug. The water was regularly replaced at regular intervals of time, and the release medium was directly analysed by HPLC to determine the released drug quantity. The results are illustrated in the Figure 22.

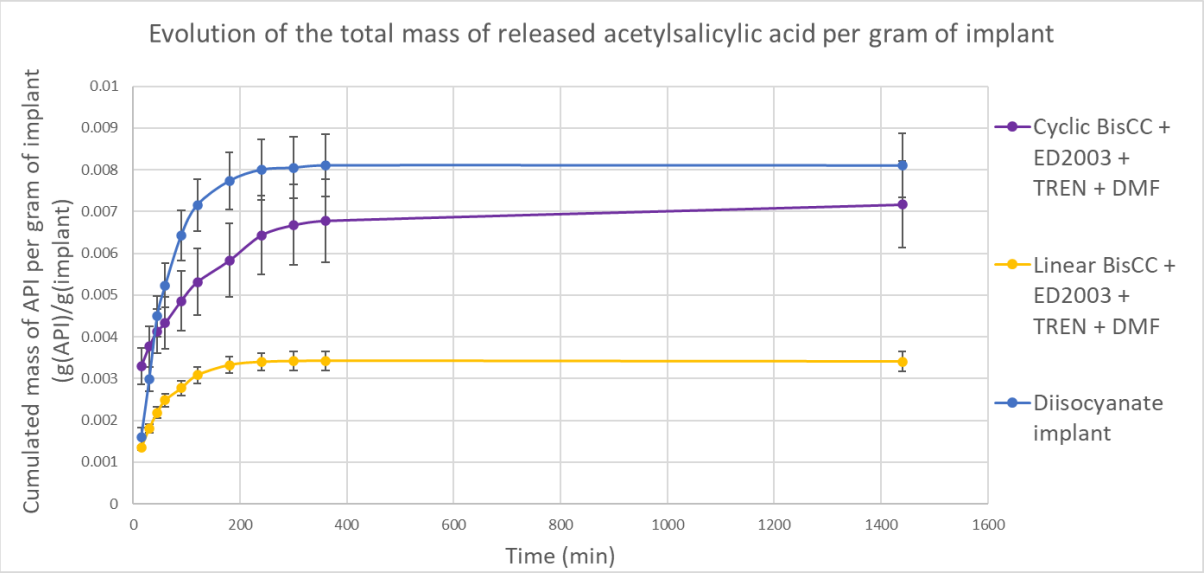

Fig. 22: Comparison of the drug-release profiles of the dried linear bis-cyclic carbonate/Jeffamine® ED2003/DMF/TREN (yellow curve) NIPU implant, the cyclic bis-cyclic carbonate/Jeffamine® ED2003/DMF/TREN (violet curve) and the isocyanate-based one (blue curve)

This comparison showed a clear difference between the NIPU implants profiles compared to the isocyanate-based implant. Although the loading conditions for all implants were the same, it appeared that the isocyanate-based one released proportionally more drug than its NIPU counterparts. This could be explained either by a higher drug-retention in the case of the NIPU implants, due to stronger interactions between the network and the API, or by a lower drug loading during the impregnation step. As mentioned in the previous section, the loading rate for each formulation was calculated based on the ceiling value in the drug-release profiles. The values are included in the Table 03.

Loading rates values			
	Linear BisCC + ED2003 + TREN + DMF	Cyclic BisCC + ED2003 + TREN + DMF	Diisocyanate implant
Mass of released API (g)	0.0002714	0.0001627	0.0003865
Mass of implant (g)	0.0796000	0.0227000	0.0477000
Loading rate (%)	0.3409896	0.7168670	0.8102848

Table 03: Loading rates of the linear bis-cyclic carbonate/ Jeffamine® ED 2003/TREN /DMF, the cyclic bis-cyclic carbonate/Jeffamine® ED 2003/TREN/DMF and the isocyanate-based implants

These results showed that the loading rate of the linear bis-cyclic carbonate-based implant is much lower than that of the isocyanate-based one, while the cyclic bis-cyclic carbonate-based implant presents a much closer value. These differences can be partly explained by the swelling rate of each formulation in DCM. Indeed, it was observed that the cyclic bis-cyclic carbonate-based implant had swelled significantly more than the linear bis-cyclic carbonate-based one. Thus, a greater amount of the API dissolved in the solvent was able to diffuse inside of the network.

Another explanation for these results is that the crosslinking for the NIPU implant may not be totally efficient (as previously hypothesized), leaving unreacted primary amine groups in addition to the central tertiary amine of the TREN. The basicity of these functions could have an impact on the acidic API leading to acid-base reactions. These reactions would prevent the release of part of the API that remains in the network, leading to lower released content, even if the loading rates were equals. It is noteworthy to mention that the release plateau is reached for a similar time for both types of hydrogels.

To compare the different formulations more effectively, the curves of the NIPU implants were normalized with the release ceiling value equal to 100%.

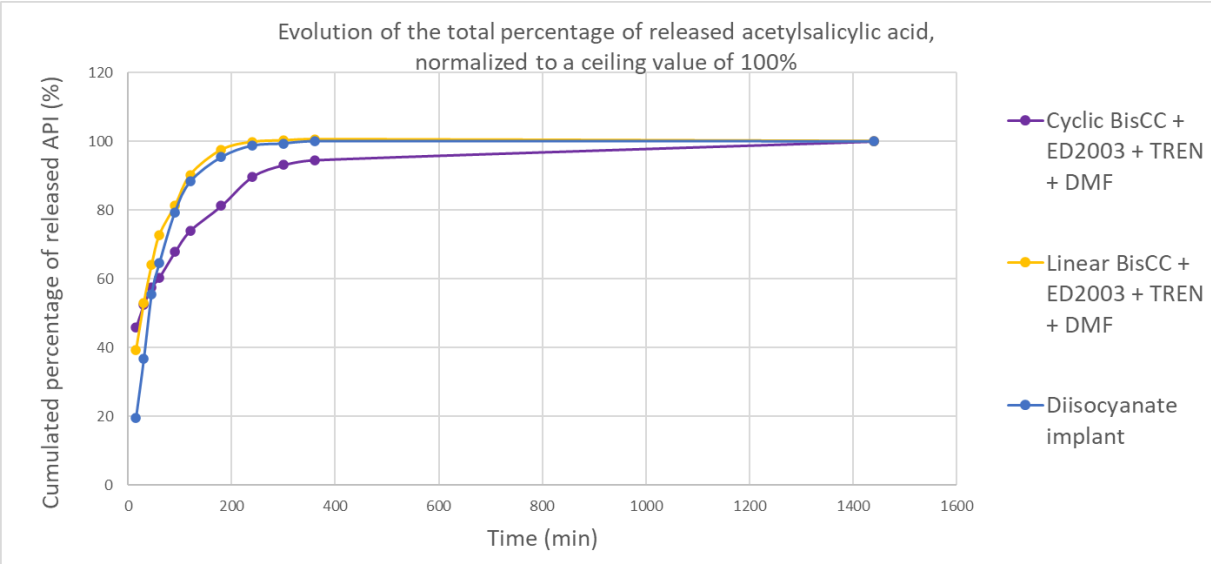

Fig. 23: Comparison of the normalized drug-release profiles of the dried linear bis-cyclic carbonate/Jeffamine® ED2003/DMF/TREN (yellow curve) NIPU implant, the cyclic bis-cyclic carbonate/Jeffamine® ED2003/DMF/TREN (violet curve) and the isocyanate-based one (blue curve)

The Figure 23 highlights the fact that, if the loading rates were equal for each formulation, the linear bis-cyclic carbonate-based implant would have a closer release profile to the isocyanate-based one than the cyclic bis-cyclic carbonate-based implant. A burst effect is

noticeable on this new graph for both the yellow and violet curves, but the yellow one quickly meets the blue curve (after 1.5 hours of release).

Mechanical properties

To assess the mechanical properties of the implant, the Young's modulus in compression was determined. Cylinders of 10 mm in diameter and 3 mm in height were cut from the washed and hydrated implants. These cylinders were then place between the plates of the compression testing bench and immersed into a water bath thermostatized at 37°C. The compression test was then performed at this temperature. A pre-load of 1N was applied to ensure that the sample was correctly placed between the compression plates before each measurement. The resulting curves are represented in the Figure 24.

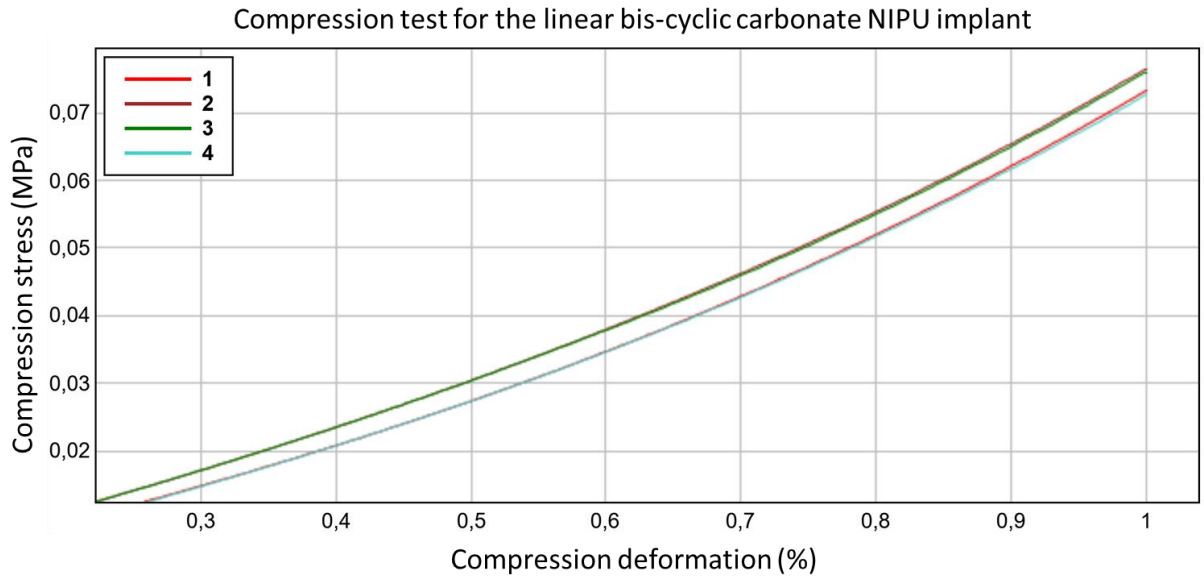

Fig. 24: Compression curves for the linear bis-cyclic carbonate-based NIPU implant

The Young's modulus was determined using the Bluehill Universal software, by calculating the slope of the linear part of these curves. The results are compiled in the Table 04.

		Young's modulus (MPa)				
		Test 1	Test 2	Test 3	Average	Standard deviation
Linear bis-CC + TREN + ED 2003 + DMF + Pre-reaction	Sample 1	8.2	8.2	8.25	8.2167	0.0289
	Sample 2	8.35	8.43	8.57	8.4500	0.1114
	Sample 3	7.47	7.52	7.63	7.5400	0.0819
Cyclic bis-CC + TREN + ED 2003 + DMF + Pre-reaction	Sample 1	162.32	164.75	166.49	164.5200	2.0945
	Sample 2	144.3	145.46	146.84	145.5333	1.2716
	Sample 3	131.75	133.87	135.63	133.7500	1.9428
Isocyanate-based Implant	Sample 1	225.32	233.3	240.59	233.0700	7.6376
	Sample 2	196.26	200.8	208.03	201.6967	5.9360
	Sample 3	179.93	184.46	192.39	185.5933	6.3068

Table 04: Young's modulus of the linear bis-bis-cyclic carbonate/Jeffamine® ED2003/TREN/ DMF, the cyclic bis-cyclic carbonate/Jeffamine® ED2003/TREN/ DMF and the isocyanate-based implants

As illustrated by the results, the Young's modulus of the linear bis-cyclic carbonate-based implant was significantly lower than for the isocyanate-based one. This translates into a less stiff implant compared to isocyanate-based hydrogels, as already observed qualitatively while handling the samples. This is in line with a network of lower crosslinking density even if the difference in chemical structure renders the comparison delicate. The implication of these results is that the NIPU implants are more sensible to compression-induced deformation than their isocyanate counterpart.

The results also validated the starting hypothesis that the transition from a linear spacer to a cyclic one would increase the stiffness of the network. Indeed, the modulus rose from an average of 8.0 MPa for the linear bis-cyclic carbonate-based implant to 147.9 MPa for the cyclic bis-cyclic carbonate-based one.

Conclusion on the impact of the bis-cyclic carbonate structure on hydrogel properties

In this part of the research, we successfully developed a formulation method of NIPU-based implants by the crosslinking of commercially available Jeffamine® by linear and cyclic bis-cyclic carbonate in presence of TREN as crosslinking agent. Depending on the structure of the bis-cyclic carbonate used, we observed a significant impact on the swelling rate and the drug-release profile. Moreover, the drug-loading was closer to the one of the isocyanate-based implant, used as reference, when switching to the cyclic bis-cyclic carbonate. The greater swelling rate reached with the cyclic bis-cyclic carbonate-based formulation could explain the increase of the drug loading as a more expended network allows for a more efficient impregnation of the polymer matrix. The difference between the drug-release profile of the NIPU implants and of the isocyanate-based one could be compensated, especially for the linear bis-cyclic carbonate-based implant, by increasing the loading rate of the NIPU implants, as suggested by the normalized release profiles. This should be confirmed by precisely determining the loading of the different hydrogels after impregnation. Concerning the mechanical properties, implants made of cyclic bis-cyclic carbonate present higher compression moduli compared to the linear-based one and are closer to the value of the isocyanate-based implant, which tend us to say that the cyclic bis-cyclic carbonate is the most appropriated candidate for the formulation of NIPU-based implants as substitutes of conventional isocyanate-based implants.

Investigation on the impact of the crosslinking agent

In the formulation protocol developed in the first part of this work, TREN proved to be an excellent crosslinking agent due to its high reactivity toward cyclic carbonate. Nevertheless, this high reactivity required an additional step. Indeed, as the amine of TREN reacted faster than the amine at both chain-ends of Jeffamine® ED2003 with the cyclic carbonate, a 4h pre-reaction between only the diamine and the bis-cyclic carbonate was required to ensure a

homogeneous crosslinking as previously discussed. Moreover, the central tertiary amine being able to be protonated in acidic conditions leads to a pH sensitivity of the network, with an impact on the swelling rate. Additionally, in the case of drug bearing acidic function, such as acetylsalicylic acid, an interaction with the network may happen with an impact on the drug release profile.

Choice of the crosslinker

To solve these issues, two commercially available triamines were considered as substitutes of TREN: the Jeffamine® T5000 (MW = 5000 g/mol) and the Jeffamine® T403 (MW = 400 g/mol) (Fig 12 D and F, respectively) that are 3-arm poly(propylene oxide) of two different molar mass, end-capped by a primary amine. Their reactivity towards the cyclic carbonate functions being similar to the linear Jeffamine® ED 2003, the pre-reaction step could be avoided. Apart from the change of the nature of the crosslinking agent, the formulation conditions remain identical to those described in the first part of this report.

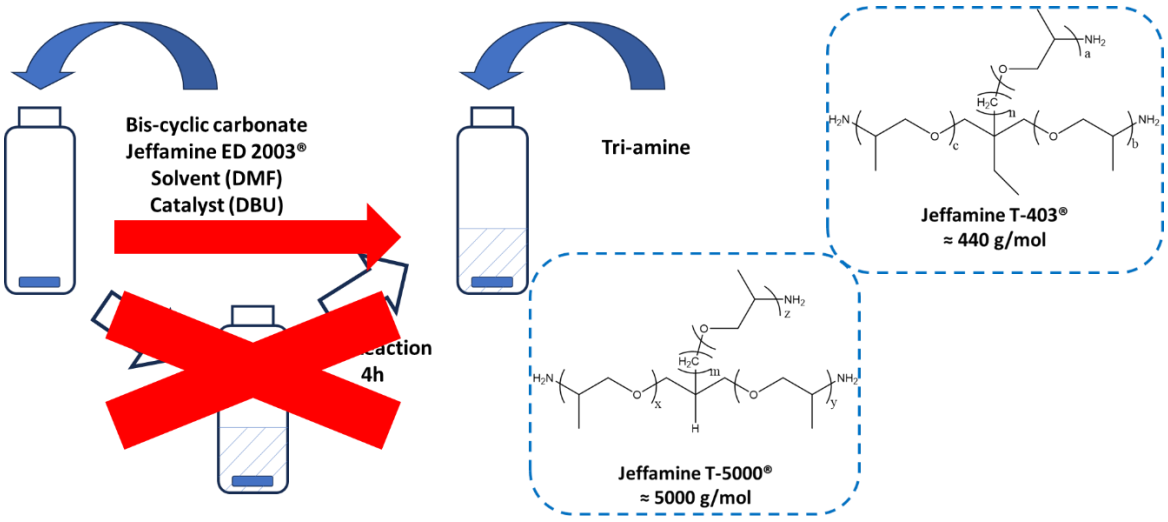

Fig. 25: NIPU formulation process with the alternative triamines

We observed that the Jeffamine® T5000 was unfortunately not miscible with the Jeffamine® ED2003 (MW = 1900 g/mol). This lack of miscibility caused all the formulations using the Jeffamine® T5000 to fail, producing a highly viscous liquid instead of a crosslinked material. Indeed, the difference in hydrophilicity of both components associated to high molar mass of the Jeffamine® T5000 leads to phase separation, preventing crosslinking to occur between both partners. This phase separation did not occur with Jeffamine® T403, which has shorter PPG chains and is thus less hydrophobic. Networks were thus synthesised by using linear bis-cyclic carbonate/Jeffamine® ED2003/DMF and dried Jeffammine® T403. The molar ratios were the same as for the TREN-based formulation using the linear bis-cyclic carbonate and the crosslinking time was kept identical in order to keep the implants comparable (1 to 3 days in the stove). The quantities of the components are included in the Table 05.

Composition of the NIPU implant				
	Linear bis-cyclic carbonate	Jeffamine® ED2003	Jeffamine® T403	DBU
m (g)	0.5828	1.1168	0.5000	0.0200
n (mol)	0.0023	0.0006	0.0011	0.0001
n functions (mol)	0.0046	0.0012	0.0034	0.0001

Table 05: Composition of the linear bis-cyclic carbonate and Jeffamine® T403-based implant

The network collected with this new crosslinker in the formulation was fully characterized and compared to TREN-based implants. The resulting implant is illustrated in the Figure 26.

Fig. 26: Liquid bis-cyclic carbonate and TREN-based implant

Swelling rate

The swelling rate of the implant was measured in water following the strategy described for TREN-based implants. The results are illustrated in the Figure 27.

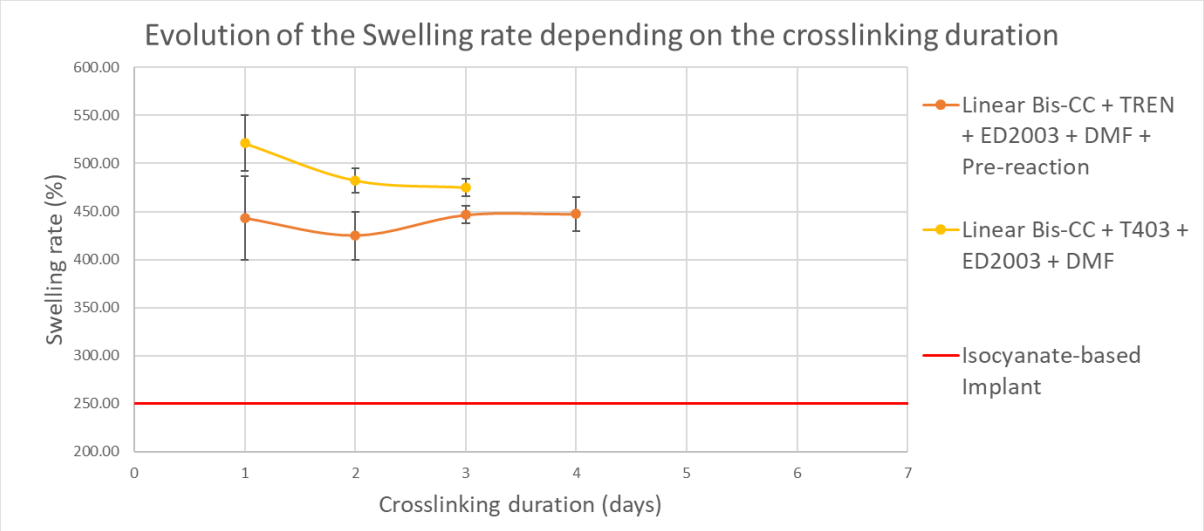

Fig 27: Comparison of the swelling degree in water of the TREN (blue) and the Jeffamine® T403(orange) -based implants with the isocyanate-based implant as reference (red)

The modification of the crosslinking agent had not a significant impact on the final swelling rate of the implant. As shown in the Figure 27, the swelling rate for the Jeffamine® T403-based implant was only monitored for three days, as it was previously determined that a longer crosslinking time did not further increase the crosslinking of the implant. When Jeffamine® T403 is used as crosslinking agent, the swelling rate is a little higher compared to the TREN-based implants of identical composition.

Based on this first analysis, the modification of the crosslinking agent was successful. Moreover, this new formulation did not include a pre-reaction step, which shortened the reaction time by four hours.

DSC

As for the previous formulations, DSC was used to determine the glass transition temperature of the Jeffamine® T403-based implant. The results are illustrated in Figure 28.

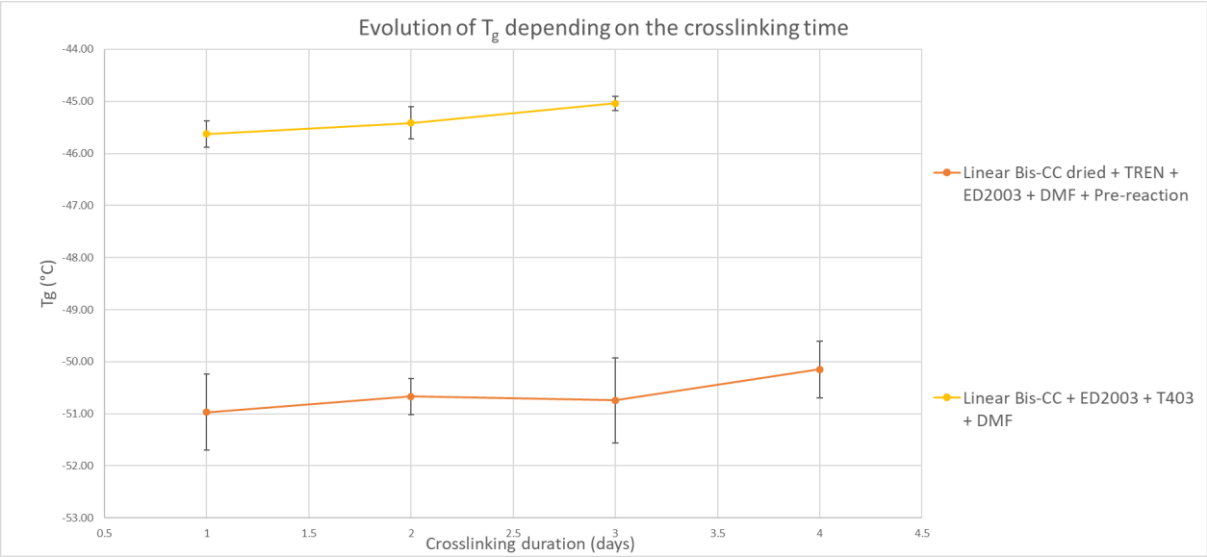

Fig. 28: Comparison of the T_g of the different implant formulations: linear bis-cyclic carbonate with TREN as crosslinking agent (orange curve) and linear bis-cyclic carbonate with Jeffamine® T403 as crosslinking agent (yellow curve)

At the opposite of swelling rate measurements, the DSC results proved that the modification of the crosslinking agent had a noticeable impact on the thermal properties of the network. Indeed, the value of T_g increased from an average of -50°C for the TREN-based to -42°C for the Jeffamine® T403-based implants. This can be explained by the increase in mass of the crosslinking agent, as its chain length increases, it has a greater impact on the thermal properties of the implant than TREN. The TREN accounted for 8.91% of the network's mass while the Jeffamine® T403 accounts for 22.73% of the implant's mass.

Drug-release profile

With the purpose to determine the impact of the use of Jeffamine® T403 on the drug loading and the release profile of acetylsalicylic acid, the impregnation process described previously was applied to the Jeffamine® T403-based implant. The results are illustrated in the Figure 29.

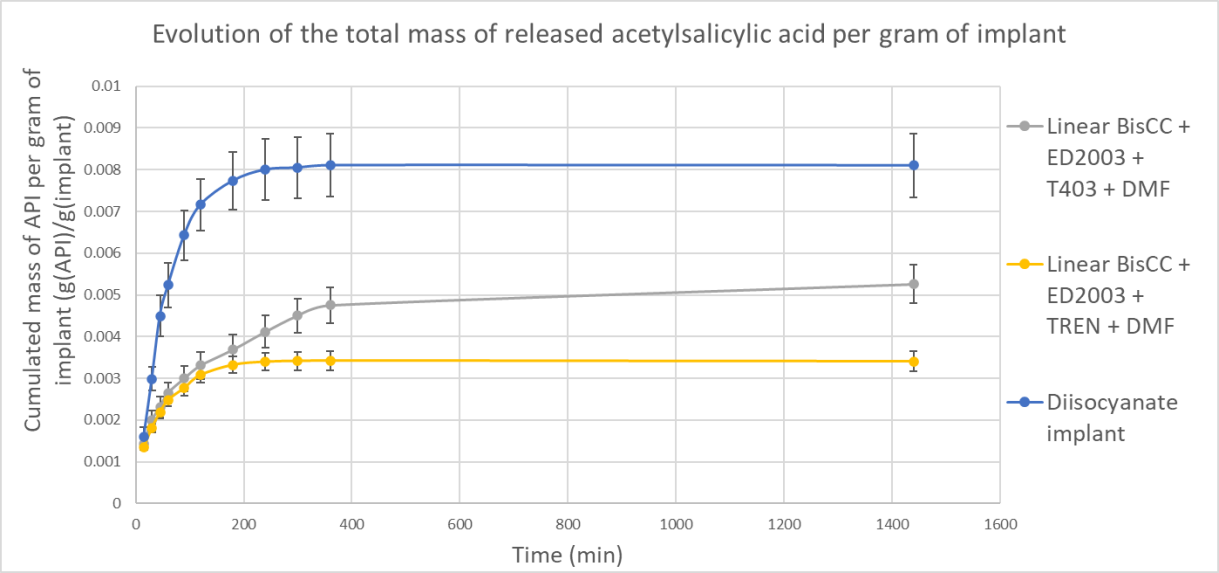

Fig. 29: Comparison between the drug release profile of the TREN-based implants (yellow), the Jeffamine® T403-based implants (grey) with the isocyanate-based formulation as reference (blue)

The results showed that the modification of the crosslinking agent induced an increase of the drug released compared to the TREN-based implant.

The absence of the central amine group in the crosslinker appears to favour the release of the API since there are no acid-base interactions in case of Jeffamine® T403-based crosslinker. This combined with the greater swelling rate in DCM (1780.53%) could explain why the release rate is higher than for the TREN-based implant. The loading rate of this formulation was calculated based on the hypothesis that the amount of released API after 24h corresponded to the total amount of loaded drug. The result is included in the Table 06 alongside previous data for comparison.

Loading rates values			
	Linear BisCC + ED2003 + TREN + DMF	Linear BisCC + ED2003 + T403 + DMF	Diisocyanate implant
Mass of released API (g)	0.0002714	0.0002378	0.0003865
Mass of implant (g)	0.0796000	0.0452000	0.0477000
Loading rate (%)	0.3409896	0.5261215	0.8102848

Table 06: Loading rates of the linear bis-cyclic carbonate/Jeffamine® ED2003/TREN/ DMF, the bis-cyclic carbonate/Jeffamine® ED2003/Jeffamine® T403/ DMF and the isocyanate-based implants

As for the TREN-based formulations, the curves were normalized to a ceiling value of 100% for a better comparison (Fig. 30).

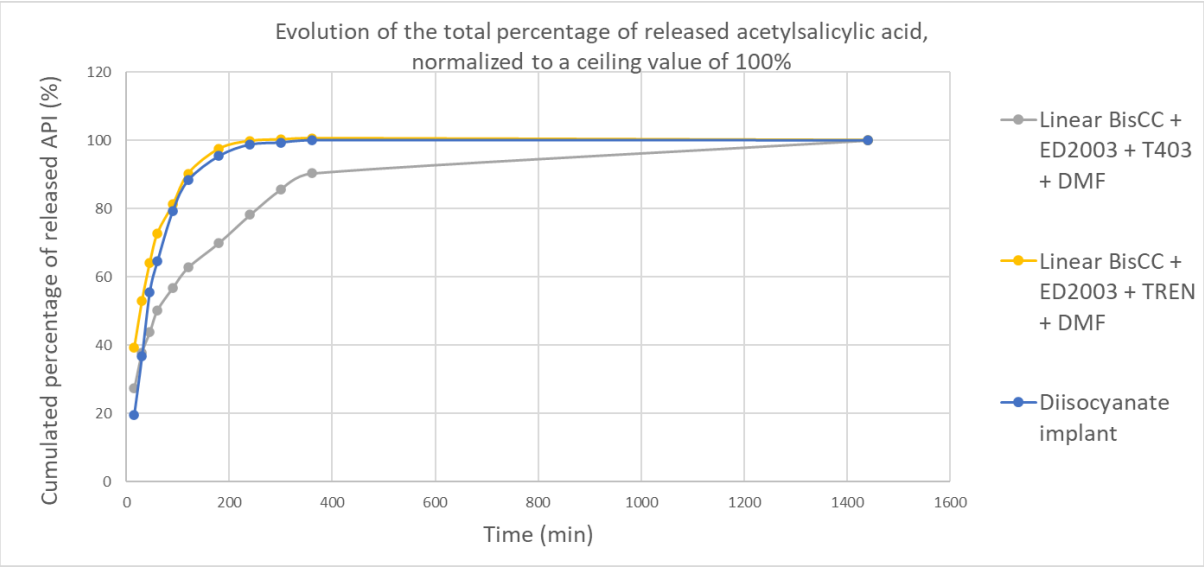

Fig. 30: Comparison between the normalized drug release profile of the TREN-based formulation (yellow), the Jeffamine® T403-based implant (grey) with the isocyanate-based formulation as reference (blue)

As illustrated by the Figure 30, the normalized release profile of the Jeffamine® T403-based implant does not correspond well to that of the isocyanate-based one. The kinetics of the release appears to be different, as the curve follows a more linear progression.

Conclusion on the impact of the crosslinking agent

Following the goal of avoiding the pre-reaction step of the initial formulation process, an implant based on the Jeffamine® T403 and on the linear bis-cyclic carbonate was successfully formulated and fully characterized. It was noted that the modification of the crosslinking agent had a remarkable impact on the thermal properties of the network. The loading and release of acid acetylsalicylic was also impacted by the change in the nature of the crosslinking agent. It was indeed observed that the Jeffamine® T403-based implant presented a greater released quantity of API than its TREN counterpart in the same loading conditions. Moreover, similarly to the impact of the transition from a linear to a cyclic bis-cyclic carbonate, the normalized release profile of the Jeffamine® T403-based formulation proved to significantly differ from the isocyanate-based one. As the release kinetics are different, this new formulation may not be fit to replace the isocyanate route. However, it potentially opens the way for new applications by widening the library of available NIPU implants.

Investigation on the liquid bis-cyclic carbonate for a solvent-free formulation process.

One of the main issues of the formulation process developed in this work is the mandatory use of DMF in order to have a liquid formulation able to be transferred in the mold. The last variation explored during this work was to test a new bis-cyclic carbonate developed in the lab, which is liquid at room temperature and thus could allow for a solvent-free crosslinking in molten state, similarly to the isocyanate route described previously. This was not possible with the previous bis-cyclic carbonates as their melting point was too close to their degradation point. Typically, this liquid bis-cyclic carbonate is characterized by an oligo(thio)ether linker and is synthesised in the laboratory according to a 3-step strategy (Fig 31).

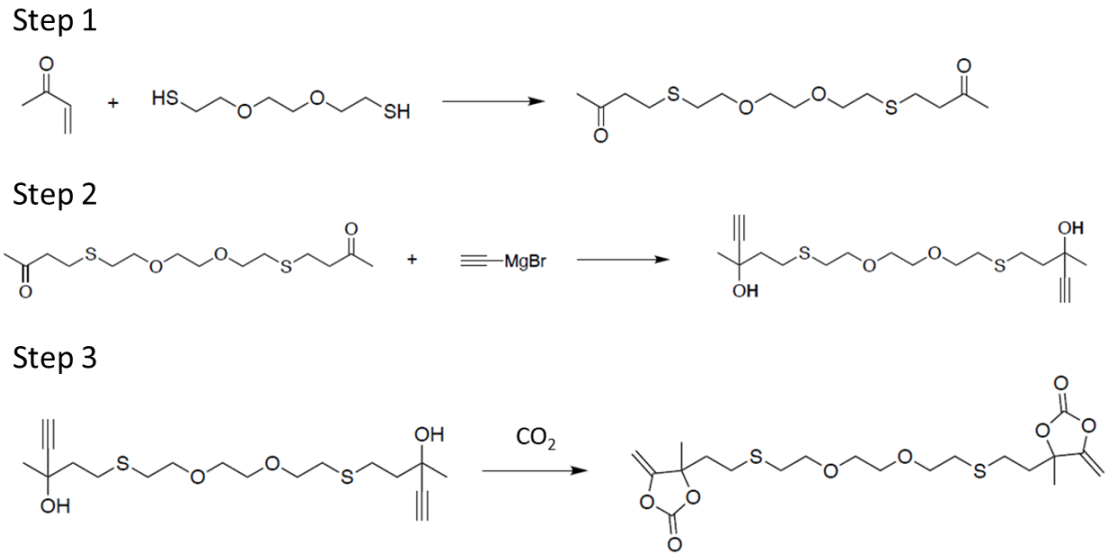

Fig. 31: Resume of the three-step synthesis of the liquid bis-cyclic carbonate

As the final product was liquid at ambient temperature, it was referred to as the "liquid bis-cyclic carbonate" throughout the manuscript.

The purity of the final product was assessed using ^{1}H NMR analysis, the spectrum is presented in Figure 32.

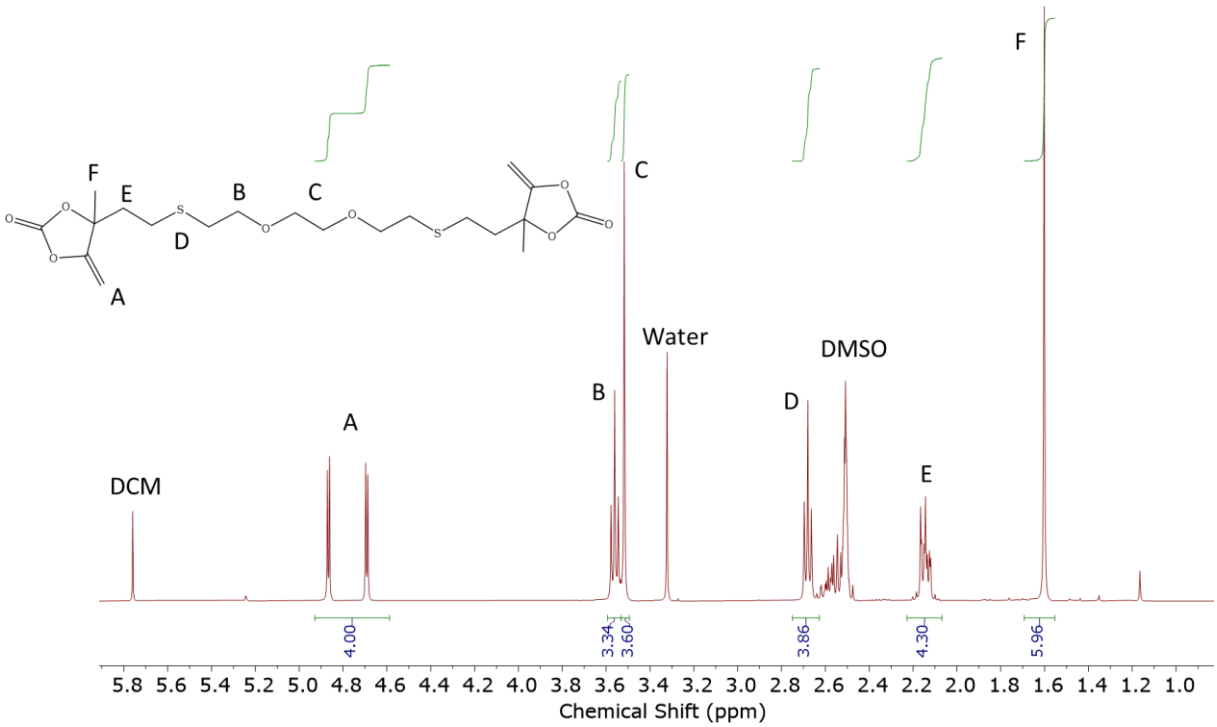

Fig. 32: ^{1}H NMR spectrum of the bis-cyclic carbonate liquid at room temperature

In this case the remaining peaks are attributed to the DMSO used as solvent for the analysis (peak at 2.54 ppm) and the water contained in the DMSO (peak at 3.33 ppm). But two other unassigned peaks are visible: one at 5.76 ppm corresponding to the DCM, and one at 2.07 ppm corresponding to the acetonitrile. Both solvents were used during the synthesis and purification of the liquid bis-cyclic carbonate, hence their presence on this spectrum.

Before testing solvent-free process, the networks were produced following the same strategy as for the first linear bis-cyclic carbonate-based implant, using 2 ml of DMF as solvent for the solubilisation of both the liquid-bis-cyclic carbonate, the Jeffamine® ED2003 and the TREN as the crosslinker, with a 4h pre-reaction step. The composition of the liquid bis-cyclic carbonate-based formulation is included in the Table 07.

Composition of the NIPU implant				
	Liquid bis-cyclic carbonate	Jeffamine® ED2003	TREN	DBU
m (g)	1.0594	1.1168	0.1662	0.0200
n (mol)	0.0023	0.0006	0.0011	0.0001
n functions (mol)	0.0046	0.0012	0.0034	0.0001

Table 07: Composition of the liquid bis-cyclic carbonate and TREN-based implant

Swelling rates

As for the previous formulations, the swelling rates of the liquid bis-cyclic carbonate-based implants were measured by immerging the implant in water for 24h before weighting them. They were then dried before the dry weight was noted. The results are represented in the Figure 33.

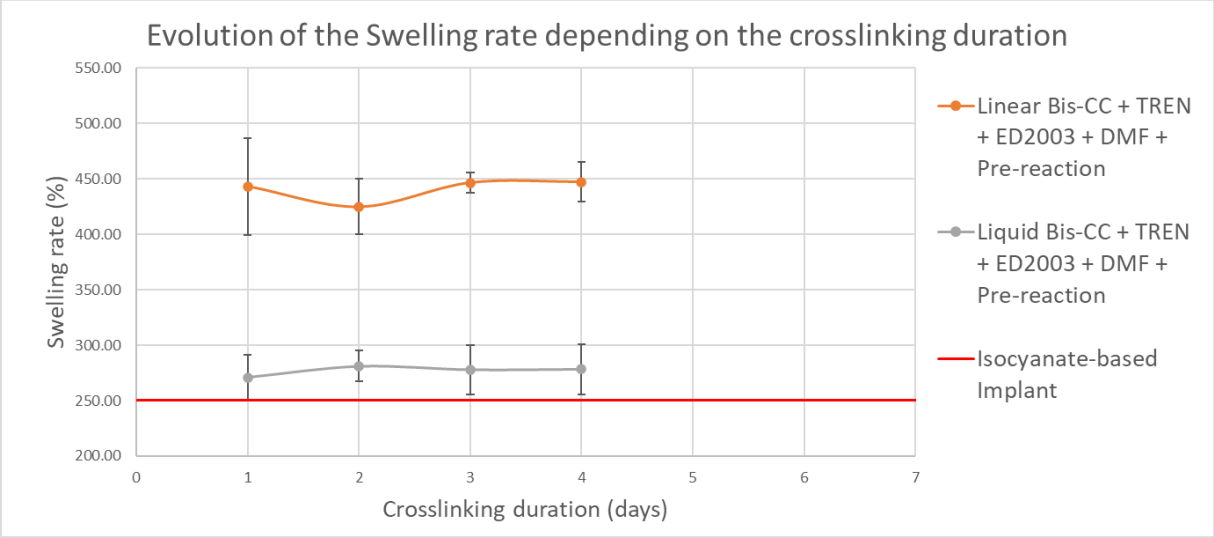

Fig. 33: Comparison of the swelling rate in water between the linear bis-cyclic carbonate-based implant (orange) and the liquid bis-cyclic carbonate-based implant (grey) with the isocyanate-based implant as reference (red)

As for the first modification of the nature of the bis-cyclic carbonate, the results indicated that the use of the liquid bis-cyclic carbonate had a noticeable impact on the swelling rate of the final implant. The swelling rate of the liquid bis-cyclic carbonate-based implant is significantly lower than for the other formulation while the ethoxy spacer is more hydrophilic than ethyl or cyclohexyl spacers. This suggests a more efficient crosslinking reaction with this flexible spacer. Moreover, the swelling rate of this new formulation is very close to that of the isocyanate-based one.

Concerning the swelling rate, the best candidate for the replacement of the isocyanate-based formulation seems to be the liquid-bis cyclic carbonate one. However, as mentioned in the previous part, a more thorough characterization is required before making any conclusion.

DSC

DSC measurements were conducted to determine the crystallinity of the implant as well as their glass transition temperature. The results are illustrated in the Figure 34.

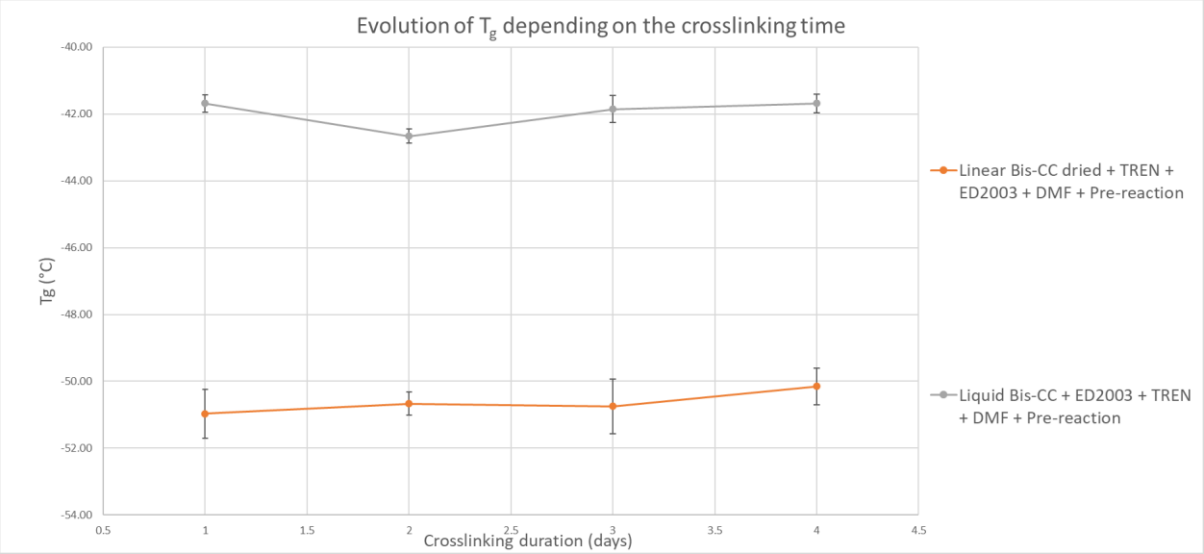

Fig. 34: Comparison of the T_g of linear bis-cyclic carbonate-based implant with TREN (orange curve) and the liquid bis-cyclic carbonate-based implant with TREN as crosslinking agent (grey curve)

These results showed that, in this case, the nature of the liquid bis-cyclic carbonate had a significant impact on the thermal properties of the network. This can be explained by the increase in molar mass of the bis-cyclic carbonate, going from 254.24 g/mol for the linear one (or 252.22 for the cyclic one) to 462.14 g/mol for the liquid one. The explanation here is similar than for the modification of the crosslinking agent. As the chain length increases, the impact on the thermal properties is greater. The increase of the Tg might also indicate a higher crosslinking density which is in line with the smaller swelling in water while increasing the hydrophilicity.

Drug-release profile

With the purpose to determine the impact of the use of liquid bis-cyclic carbonate on the drug loading and the release profile of acetylsalicylic acid, the impregnation process described previously was applied to the liquid bis-cyclic carbonate-based implant and the release was realized with the same protocol used for linear bis-cyclic carbonate-based implants. The results are illustrated in the Figure 35.

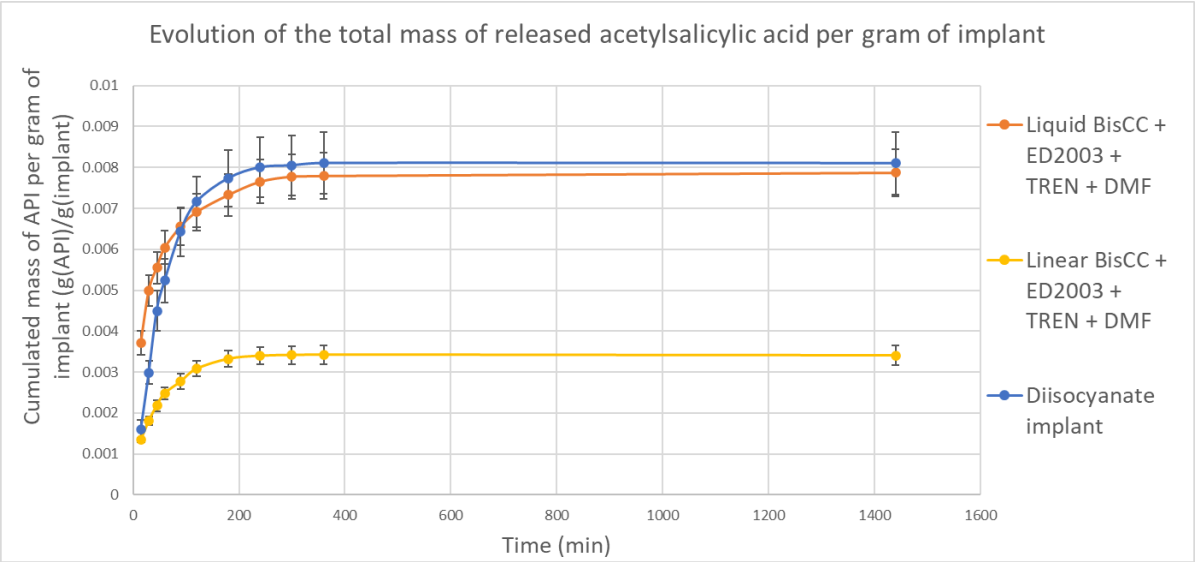

Fig. 35: Comparison between the drug release profiles of the linear bis-cyclic carbonate and TREN-based implant (yellow), the liquid bis-cyclic carbonate and TREN-based implant (orange) with the isocyanate-based implant as reference (blue)

As observed the Figure 35, the drug-release ceiling is higher in case of the liquid bis-cyclic carbonate formulation while the swelling in water was found lower than for the linear bis-cyclic carbonate network. The better crosslinking could lead to less free unreacted amine in the network and thus less interaction with the acidic drug. Besides, the ether spacer would decrease the hydrophobic interaction with the aromatic ring of acetylsalicylic acid. These could explain the larger release observed for this network even if it appears more densely crosslinked than the others. These results also suggested that the liquid bis-cyclic carbonate-based implant was the best candidate for the replacement of the isocyanate-based implant. However, a burst effect is observed at the beginning of the curve, meaning that the NIPU implant releases the encapsulated drug faster than its isocyanate counterpart at the start of the experiment.

At this point of the research, it is difficult to conclude on the impact of this phenomenon on the viability of the NIPU implant as a candidate. Indeed, this effect may be observable for the acetylsalicylic acid but not for other APIs. Moreover, each of these two curves are located within the error range of the other. Those error bars represent the standard deviation observed for each measurement. As the curve represents the evolution of the total released mass, the error bars were calculated following the error propagation theory.

The loading rate of this formulation was calculated using the total amount of released drug after 24h as if it was the total mass of loaded drug in the polymer matrix. The result is included in the Table 08 below, alongside previously calculated values for comparison.

Loading rates values			
	Linear BisCC + ED2003 + TREN + DMF	Liquid BisCC + ED2003 + TREN + DMF	Diisocyanate implant
Mass of released API (g)	0.0002714	0.0002559	0.0003865
Mass of implant (g)	0.0796000	0.0325000	0.0477000
Loading rate (%)	0.3409896	0.7873707	0.8102848

Table 08: Loading rates of the linear bis-cyclic carbonate/Jeffamine® ED2003/TREN/ DMF, the liquid bis-cyclic carbonate/Jeffamine® ED2003/TREN/ DMF and the isocyanate-based implants

This Table shows that the loading rate of liquid bis-cyclic carbonate-based formulation is the closest compared to the isocyanate-based implant yet. It confirms the fact that this formulation is promising for the replacement of the isocyanate-based one as it presents similar drug-loading and drug-release properties for the same drug-loading conditions.

Solvent-free formulation process

The next step was to investigate the solvent-free formulation. For this purpose, the liquid bis-cyclic carbonate was mixed with the diamine, and both were melted at 30°C. The catalyst was added to the mixture which was then stirred under inert atmosphere for 4 hours. The TREN was then added to initiate the crosslinking step. This last step was successful, but the reaction speed proved to be harder to control than expected. Indeed, the mixture set inside the vial just after the addition of the TREN.

To counter this issue, several attempts were made to slow the reaction rate by lowering the amount of catalyst in the mixture. However, due to a lack of time, the optimization of this formulation could not be completed during the duration of this master thesis.

Mechanical properties

The last step of this work was a global comparison of the Young's modulus in compression of all the formulated hydrogels recorded in water at 37°C. The results are summarized in the following table.

		Young's modulus (MPa)				
		Test 1	Test 2	Test 3	Average	Standard deviation
Linear bis-CC + TREN + ED 2003 + DMF + Pre-reaction	Sample 1	8.2	8.2	8.25	8.2167	0.0289
	Sample 2	8.35	8.43	8.57	8.4500	0.1114
	Sample 3	7.47	7.52	7.63	7.5400	0.0819
Cyclic bis-CC + TREN + ED 2003 + DMF + Pre-reaction	Sample 1	162.32	164.75	166.49	164.5200	2.0945
	Sample 2	144.3	145.46	146.84	145.5333	1.2716
	Sample 3	131.75	133.87	135.63	133.7500	1.9428
Isocyanate-based Implant	Sample 1	225.32	233.3	240.59	233.0700	7.6376
	Sample 2	196.26	200.8	208.03	201.6967	5.9360
	Sample 3	179.93	184.46	192.39	185.5933	6.3068
Cervidil® implant	Sample 1	200.41	203.05	205.36	202.9400	2.4768
	Sample 2	216.53	218.44	225.57	220.1800	4.7646
	Sample 3	211.16	213.29	214.28	212.9100	1.5943
Linear Bis-CC + T403 + ED 2003 + DMF	Sample 1	8.13	7.68	8.61	8.1400	0.4651
	Sample 2	6.19	6.45	4.8	5.8133	0.8871
	Sample 3	8.86	9.21	9.25	9.1067	0.2146
Liquid Bis-CC + TREN + ED 2003 + DMF + Pre-reaction	Sample 1	40.62	41.86	42.72	41.7333	1.0557
	Sample 2	38.83	39.12	39.84	39.2633	0.5200
	Sample 3	44.23	44.39	44.75	44.4567	0.2663

Table 09: Young's modulus of the different tested implants

Here, we tested all the NIPU formulations as well as both our own isocyanate-based implant and the commercially available Cervidil® one. Dixon tests were conducted on the series of measures to eliminate potentially abhorrent values, but none required to be ignored. The results proved that the Young's modulus is highly dependent on the nature of the bis-cyclic carbonate when comparing the NIPU formulations. Indeed, it greatly differs between the linear one and the liquid one for example but stays roughly the same between the two linear bis-cyclic carbonate-based ones. In all cases, the NIPU implant present lower Young's modulus than the isocyanate-based ones, making them more sensible to deformation. This table also shows that the goal of increasing the stiffness of the network by replacing the linear bis-cyclic carbonate by the cyclic one proved to be successful, as it greatly increased the Young's modulus. The higher modulus observed for the liquid bis-cyclic carbonate as compared to the linear one is in line with a higher crosslinking density for this hydrogel.

Conclusion of the liquid bis-cyclic carbonate formulations part

With the purpose to avoid the presence of any organic solvent in the formulation mixture, the liquid bis-cyclic carbonate was successfully synthesised and proved to be as effective for the efficient crosslinking in DMF of Jeffamine® ED 2003 in presence of TREN as crosslinking agent compared to the two other bis-cyclic carbonates (linear and cyclic) used in the beginning of this work. Remarkably, the liquid bis cyclic carbonate has a significant impact on the thermal and physico-chemical properties of the implants as testified by the DSC and mechanical properties analyses. Moreover, an increase of the encapsulation efficiency in the case of acetylsalicylic acid was observed comparable to the one obtained with isocyanate-based implant.

Nevertheless, several solvent-free formulations were carried out, but the crosslinking is hard to control, resulting in the solution setting in the vial before it could be poured into the molds. Even if this goal was not completely reached during this master thesis, we proved that the solvent-free formulation was accessible, albeit more uphill than expected.

General Conclusion

During this research, we were able to successfully developpe synthetic routes for the formulation of Non-Isocyanate Poly-Urethane networks as potential candidates for the replacing of commercially available isocyanate-based formulation. The first formulation used a linear bis-cyclic carbonate with Jeffamine® ED2003 dissolved in DMF, and TREN as a crosslinking agent. The comparison of the collected implant with the isocyanate-based implant highlighted a clear difference regarding the physico-chemical properties, notably in the drug-release profile and the swelling rate. Alternative formulations were then investigated with different bis-cyclic carbonates or different crosslinking agent. A total of four formulations were developped and fully characterized: the linear bis-cyclic carbonate with TREN; the cyclic bis-cyclic carbonate with TREN; the liquid bis-cyclic carbonate with TREN and the linear bis-cyclic carbonate with Jeffamine® T403. In all cases, the formulated implants can be loaded by an active principle, namely acetylsalicylic acid, according to an impregnation procedure with a release dependent of the composition.

Out of all these options, the liquid bis-cyclic carbonate-based one presented the closest specifications to the isocyanate-based implant and is at the time the most promising formulation although it stills differing in certain points such as the value of the Young's modulus or the burst effect observed at the start of the drug release.

Nevertheless, we were able to create a library of NIPU formulations, each having its own set of properties for drug-release applications. Moreover, although it still needs to be optimized, we were successful in developing a solvent-free NIPU formulation, thus solving the issue of the solvent's toxicity.

Perspectives

The first perspective is the optimization of the solvent-free formulation. Indeed, were able to produce a network using the liquid-bis-cyclic carbonate together with the Jeffamine® ED2003 in a molten state by adding the TREN directly to the mixture, but the reaction rate was too fast, and we could not pour the mixture in the molds before it set. Subsequent tries were attempted, during which we lowered the amount of catalyst in order to slow down the reaction, but the perfect ratio was not determined, and the reaction kept being either too fast, either too slow.

Secondly, even if the present report focuses on four formulation routes, other formulations were envisaged during the research. Typically, we tried to substitute the TREN for the formulations based on both cyclic and liquid bis-cyclic carbonate. Thus, we were able to produce networks made from the cyclic bis-cyclic carbonate and the Jeffamine® T403; or the liquid bis-cyclic carbonate and the Jeffamine® T403. However, we encountered some issues during this part of the project, which ultimately made it impossible for us to fully characterize those additional formulations in time. We still observed the feasibility of these formulations, even if they need more optimizations than the previous ones. The liquid bis-cyclic carbonate and Jeffamine® T403 one would be particularly interesting to characterize as it could solve both the solvent issue and the pre-reaction issue at the same time.

We would also like to precisely determine the loading rate of the implants. The discussions in this manuscript are based on the hypothesis that the total amount of released drug after 24h of release corresponds to the quantity of encapsulated drug. However, we know that this may not be the case as acid-base reactions can take place between the carboxylic acid of the API and the free non-reacted amines of the network. Thus, the precise quantification of the number of free amine functions inside the polymer network would also help in the understanding of the diverse phenomenon taking place during the loading step. The investigation of the potential of these new NIPU-based implants for the encapsulation and the release of another active principle could increase the potential application field of the developed formulations.

Finally, it would have been interesting to change the molar ratio of the components in the NIPU formulations, to observe the impact on the crosslinking density of the network and on the different properties of the implant.

Materials and methods

Reactants

Linear and cyclic bis-cyclic carbonates

The syntheses of the linear and cyclic bis-cyclic carbonates were achieved based on the work of S. Gennen et al[39].

Typically, 800 ml of a solution of ethynyl magnesium bromide in THF (0.5 M) was distilled under vacuum to reduce the solvent volume by 300 ml. 0.13 mol of diketone (14.8 g for linear and 14.6 g for cyclic bis-cyclic carbonate) was dissolved in a minimum volume of anhydrous tetrahydrofuran before being added dropwise to the ethynyl magnesium bromide solution under inert atmosphere in an ice bath to prevent overheating. The solution was then left to react overnight under stirring before being quenched by the addition of 260 mL of an aqueous saturated ammonium chloride solution. After decantation, solution was diluted with 300 mL of diethylether and the organic phase was extracted through a liquid-liquid extraction using diethyl ether as the organic solvent (3 x 300 mL). The extracted phase was then dried using anhydrous magnesium sulphate and filtrated before the evaporation of the solvent under vacuum. The white solid collected was then dissolved in diethyl ether and purify by flash column chromatography using the same solvent as eluant. The column was packed with silica powder and was meant to retain the impurities hypothetically present in the solution. The mobile phase was collected in a round bottomed flask and the solvent was evaporated to obtain a white solid.

The powder collected at the end of the first step (20 g; 0.12 mol) was then dissolved in acetonitrile (40 mL) with copper iodide (1.15 g; 6 mmol) and tetrabutylammonium phenolate (2 g; 6 mmol) as catalysts. The solution was poured in a reactor (250 mL), which was then pressurized to 100 bar using carbon dioxide and put to 40°C under stirring overnight (330 rpm). The reactor was then depressurized, and the content was recovered using dichloromethane (400 mL) to dissolve the solid formed during the reaction. The recovered solution was once again purified on a silica column using dichloromethane as eluant. The mobile phase was collected in a round bottomed flask and the solvent was evaporated under vacuum, yielding a yellow solid. After being dried under vacuum, this solid was recrystalized using acetonitrile (300 mL) as a solvent by lowering the temperature to -20°C for 24h. A white solid was then recovered by filtration before being dried under vacuum and kept in a desiccator before use (yield: 90% for the cyclic bis-cyclic carbonate; 90% for the linear bis-cyclic carbonate).

Liquid Bis-cyclic carbonate

Methyl vinyl ketone (25.2 g; 0.36 mol), freshly distilled under vacuum, was dissolved in chloroform (25 mL) and added dropwise in an ice bath to a solution of diether dithiol (28.7 g; 0.15 mol) in chloroform (125 mL) with DBU (456 mg; 3 mmol) as catalyst. The reaction was driven in air for 2h at room temperature before being quenched by the addition of a large volume of chloroform (450 mL). The organic phase was then extracted using water (3 x 300 mL) as the solvent and dried with anhydrous magnesium sulphate and filtered. The solvent was then evaporated while adding portions of hexane to form an azeotrope with the chloroform.

Once the diketone was synthesised, the rest of the method was the same as for the other bis-cyclic carbonates. 800 ml of a solution of ethynyl magnesium bromide in THF (0.5 M) was distilled under vacuum to reduce the solvent volume by 300 ml. 0.13 mol of diketone (41.86 g) was dissolved in a minimum volume of anhydrous tetrahydrofuran and added dropwise to the ethynyl magnesium bromide solution under inert atmosphere in an ice bath to prevent overheating. The solution was then left to react overnight under stirring before being quenched by the addition of 260 mL of an aqueous saturated ammonium chloride solution. After decantation, solution was diluted with 300 mL of diethylether and the organic phase was extracted through a liquid-liquid extraction using diethyl ether as the organic solvent (3 x 300 mL). The extracted phase was then dried using anhydrous magnesium sulphate and filtrated before the evaporation of the solvent under vacuum. The collected oil was then dissolved in diethyl ether and purify by flash column chromatography using the same solvent as eluant. The column was packed with silica powder and was meant to retain the impurities hypothetically present in the solution. The mobile phase was collected in a round bottomed flask and the solvent was evaporated to obtain a viscous yellow oil.

The oil from the precedent step (20 g; 0.062 mol) was then dissolved in acetonitrile (10.7 mL) with copper iodide (0.508 g; 2.675 mmol) and DBU (0.407 g; 2.675 mmol) as catalysts. The solution was poured in a reactor (250 mL), which was then pressurized to 40 bars using carbon dioxide and put to 40°C under stirring overnight (330 rpm). The reactor was then depressurized, and the content was recovered using a mixture 80/20 in volume of dichloromethane/diethyl ether (400 mL) to dissolve the oil formed during the reaction. The recovered solution was once again purified on a silica column using the same mixture as eluant. The mobile phase was collected in a round bottomed flask and the solvent was evaporated under vacuum, yielding a yellow oil. It was then left under normal atmosphere for 24h to allow the copper to oxidize before being diluted in 400 mL in DCM and stirred in presence of Chelex® resin (200 mg/g of monomer) to complex the copper. The solution was then filtered, and the solvent was evaporated under vacuum under stirring. The obtained viscous oil was then kept in a desiccator under vacuum (yield = 95%).

Commercially available reactants

Jeffamine® ED2003 was purchased by Sigma-Aldrich. It was used either as received, dried under vacuum, or freeze-dried depending on the formulation. Jeffamine® T403 and Jeffamine® T5000 were kindly provided by Huntsman and used either as received or purified by azeotropic distillation using toluene as the solvent. Tris(2-aminoethyl) amine (TREN); Ethynyl magnesium bromide; α,ω-dihydroxyl-PEO; 1,2,3-hexanetriol; dibutyltin dilaurate; di-cyclohexyl diisocyanate; ammonium chloride and tetrabutylammonium bromide were purchased by Sigma-Aldrich and used as received. Magnesium sulphate was purchased by VWR and used as received. 1,4-cyclohexanedione was purchased by Fluorochem and used as received. DBU was purchased by Janssen and used after a vacuum distillation.

Implants formulation

Isocyanate-based implants

25 g (6.25 mmol of hydroxyl groups) of α,ω-dihydroxyl-PEO, dried overnight under vacuum, was melted in a reaction tube before adding 1.25 g (27.95 mol of hydroxyl groups) of 1,2,6-hexanetriol and a drop of dibutyltin dilaurate as catalyst (0.03376 mmol). The solution was mixed for a few minutes before being dried under vacuum until no bubbles were visible. 4.5 g (34.31 mmol of isocyanate groups) of dicyclohexyldiisocyanate were then added under stirring to the solution which was then swiftly poured into a specific mold that was put in a heated press at 90°C for 2h. After that, the mold was moved to an oven at 90°C under a load overnight. This method produces sheets of crosslinked material from which the implants can then be cut, as illustrated by the of hydroxyl groups.

Fig. 36: Isocyanate-based polyurethane implants

Bis-Cyclic carbonates route

Linear bis-cyclic carbonate and TREN-based formulation process

The networks were prepared by dissolving 0.5828 g (0.004585 mol of cyclic carbonate) of the dried linear bis-cyclic carbonate with 1.12 g (0.001176 mol of amine) of the freeze-dried Jeffamine® ED2003 in 2 ml of anhydrous dimethylformamide (DMF). 0.02 mL of DBU (0.0001314 mol) was then added as a catalyst and the solution was stirred under inert atmosphere for 4h at 30°C. 0.17 g (0.003409 mol of amine) of TREN were then added to the solution which was then poured into the implant-shaped molds. The molds were then placed in an oven at 90°C for 2 days to complete the crosslinking of the material.

Cyclic bis-cyclic carbonate and TREN-based formulation process

0.5782 g (0.004585 mol of cyclic carbonate) of the dried cyclic bis-cyclic carbonate with 1.12 g (0.001176 mol of amine) of the freeze-dried Jeffamine® ED2003 were dissolved in 2 ml of anhydrous dimethylformamide (DMF). 0.02 mL of DBU (0.0001314 mol) was then added as a catalyst and the solution was stirred under inert atmosphere for 4h at 30°C. 0.17 g (0.003409 mol of amine) of TREN were then added to the solution which was then poured into the implant-shaped molds. The molds were then placed in an oven at 90°C for 2 days to complete the crosslinking of the material.

Liquid bis-cyclic carbonate and TREN-based formulation process

1.0594 g (0.004585 mol of cyclic carbonate) of the dried liquid bis-cyclic carbonate with 1.12 g (0.001176 mol of amine) of the freeze-dried Jeffamine® ED2003 were dissolved in 2 ml of anhydrous dimethylformamide (DMF). 0.02 mL of DBU (0.0001314 mol) was then added as a catalyst and the solution was stirred under inert atmosphere for 4h at 30°C. 0.17 g (0.003409 mol of amine) of TREN were then added to the solution which was then poured into the implant-shaped molds. The molds were then placed in an oven at 90°C for 2 days to complete the crosslinking of the material.

Linear bis-cyclic carbonate and Jeffamine® T403-based formulation process

0.5828 g (0.004585 mol of cyclic carbonate) of the dried linear bis-cyclic carbonate with 1.12 g (0.001176 mol of amine) of the freeze-dried Jeffamine® ED2003 were dissolved in 2 ml of anhydrous dimethylformamide (DMF). 0.02 mL of DBU (0.0001314 mol) was then added as a catalyst and the solution was stirred under inert atmosphere for 4h at 30°C. 0.5 g (0.003409 mol of amine) of Jeffamine® T403 were then added to the solution which was then poured into the implant-shaped molds. The molds were then placed in an oven at 90°C for 2 days to complete the crosslinking of the material.

Drug impregnation

The implants were loaded by swelling in a solution 0.2 g/L of acetyl salicylic acid in dichloromethane for 2 hours. The implants were then dried overnight under a hood before being vacuum-dried for 2 hours.

Drug release

The acetyl salicylic acid-loaded implants were immerged in 2 ml of Ultrapure® water and placed in an incubator at 37°C to start the release. At regular periods of time, the water was entirely replaced by a fresh volume of 2 ml.

Analytic methods

Swelling Rate

The swelling rates were measured by submerging the implant in 10 mL of Ultrapure® water for 24h. The weight was determined by gravimetry, and the implant was left to dry overnight under a hood before being vacuum-dried an additional night. The dry weight of the implant was then determined by gravimetry. The swelling rate was then calculated using the following formula:

$$Swelling\ (\%) = \frac{m_{swelled} - m_{dried}}{m_{dried}} * 100$$

Nuclear Magnetic Resonance

All the ^{1}H NMR analyses were conducted using an Advance III 400 MHz Bruker (liquid phase). The samples were prepared by dissolving 10 mg of the product in 700 µL of the appropriate deuterated solvent. The obtained spectra were analysed using the MNova® software.

High Precision Liquid Chromatography

Equipment

The HPLC equipment is composed of a Waters Autosampler 2707; a Waters Controller 600 and a Waters PDA 996. The column was a Polaris C18-A packed with particles which size was 0.5 µm, the length of the column was of 250 mm and its diameter of 4.6 mm.

HPLC samples preparation

Each sample of the release measurement water was then diluted by 2 ml of acetonitrile before being filtered on 0.2 µm Millipore® filters. The filtered samples were then transferred in an injection vial and placed in the injection rack of the HPLC injector.

HPLC method

The samples were analysed in triplicates, each injection consisted of a 20 µL volume and was performed at 30°C, the run time was set to 5 min and the detection wavelength was 275 nm. The mobile phase consisted of a solution of H_3PO_4/H_2O/Acetonitrile in a 4/400/600 volume ratio in an isocratic mode.

Calibration curve

The calibration curve was obtained by analysing several solutions of known concentrations. The stock solution was prepared by dissolving 5 mg of acetylsalicylic acid in 10 mL of a mix 60/40 in volume of water and acetonitrile. The other solutions were prepared by dilution of the stock solution in the same mixture of solvents. In total, 6 solutions were prepared: 0.5; 0.1; 0.05; 0.025; 0.0025 and 0.00125 g/L of acetylsalicylic acid. The elution peak of the API was measured after a retention time of 3 minutes. The calibration curve is represented in the Figure 37.

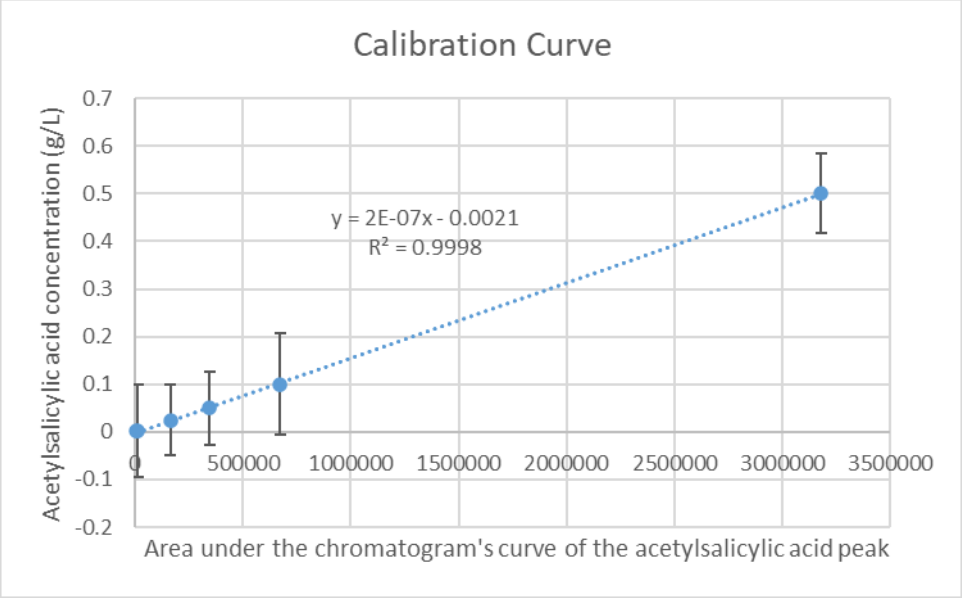

Fig. 37: Calibration curve for acetylsalicylic acid quantification by HPLC

Differential Scanning Calorimetry

The measurements were conducted on a TA Instrument DSC250. Samples of 3 to 5 mg were cut from the washed and dried implant before being weighted and placed inside closed metallic pans, which was then placed in the autosampler of the machine. Each implant was analysed in triplicate. The analysis began with a cooling step to -80°C, before a first ramp of heating of 1°C/min was applied up to 100°C. This first heating ramp was not analysed as it served to clear the thermic history of the sample. A second cooling ramp of -1°C/min was then applied to the sample down to -80°C. Finally, a second heating ramp of 1°C/min was applied until 100°C was reached. It is on this last ramp that the values were calculated using the TRIOS software.

Compression tests

The measurements were conducted on a Instron bench model 34TM-10 equipped with a BioPuls® thermostatic water bath. Circular samples were cut from the washed and hydrated implant before their height and diameter were precisely measured using an electronic vernier from Fowler®. Each implant was analysed in triplicates.

The sample was then place on the lower compression plate, the upper compression plate was moved down until it touched the sample and locked it in place. The thermic bath set to 37°C was then lifted to submerge the compression plates and the sample. A pre-load of 1N was applied to the sample in order to assure that it was correctly placed on the surface of the compression plates. The test then began, with a displacement of the upper plate set to 1 mm/min. The test was set to end when either the displacement reached 1 mm or the applied force reached 10 N, in order to keep the sample from total loss. For each triplicate of a single implant, 4 tests were performed. The first one was never used in the calculation as it served as a training test during which the sample was correctly place between the plates. The three subsequent tests were analysed using the Bluehill Universal software to determine the Young's modulus in compression.

Bibliography

(1) Embrey, M. P.; Graham, N. B.; Mcneil1, M. E.; Hillier, K. *LN VITRO RELEASE CHARACTERISTICS AND LONG TERM STABILITY OF POLY(ETHYLENE OXIDE) HYDROGEL VAGINAL PESSARIES CONTAINING PROSTAGLANDIN E*.

(2) Quarterman, J. C.; Geary, S. M.; Salem, A. K. Evolution of Drug-Eluting Biomedical Implants for Sustained Drug Delivery. *European Journal of Pharmaceutics and Biopharmaceutics* **2021**, *159*, 21–35. https://doi.org/10.1016/j.ejpb.2020.12.005.

(3) Fayzullin, A.; Bakulina, A.; Mikaelyan, K.; Shekhter, A.; Guller, A. Implantable Drug Delivery Systems and Foreign Body Reaction: Traversing the Current Clinical Landscape. *Bioengineering*. MDPI December 1, 2021. https://doi.org/10.3390/bioengineering8120205.

(4) Ahmed, K. K.; Tamer, M. A.; Ghareeb, M. M.; Salem, A. K. Recent Advances in Polymeric Implants. *AAPS PharmSciTech*. Springer New York LLC October 1, 2019. https://doi.org/10.1208/s12249-019-1510-0.

(5) Shapira-Furman, T.; Serra, R.; Gorelick, N.; Doglioli, M.; Tagliaferri, V.; Cecia, A.; Peters, M.; Kumar, A.; Rottenberg, Y.; Langer, R.; Brem, H.; Tyler, B.; Domb, A. J. Biodegradable Wafers Releasing Temozolomide and Carmustine for the Treatment of Brain Cancer. *Journal of Controlled Release* **2019**, *295*, 93–101. https://doi.org/10.1016/j.jconrel.2018.12.048.

(6) Caló, E.; Khutoryanskiy, V. V. Biomedical Applications of Hydrogels: A Review of Patents and Commercial Products. *European Polymer Journal*. Elsevier Ltd 2015, pp 252–267. https://doi.org/10.1016/j.eurpolymj.2014.11.024.

(7) Katz, G.; Harchandani, B.; Shah, B. Drug-Eluting Stents: The Past, Present, and Future. *Current Atherosclerosis Reports*. Current Medicine Group LLC 1 March 1, 2015. https://doi.org/10.1007/s11883-014-0485-2.

(8) Williams, D. F. On the Mechanisms of Biocompatibility. *Biomaterials* **2008**, *29* (20), 2941–2953. https://doi.org/10.1016/j.biomaterials.2008.04.023.

(9) Jamaledin, R.; Makvandi, P.; Yiu, C. K. Y.; Agarwal, T.; Vecchione, R.; Sun, W.; Maiti, T. K.; Tay, F. R.; Netti, P. A. Engineered Microneedle Patches for Controlled Release of Active Compounds: Recent Advances in Release Profile Tuning. *Advanced Therapeutics*. Blackwell Publishing Ltd December 1, 2020. https://doi.org/10.1002/adtp.202000171.

(10) Novel Materials for Controlled Peptide Delivery: Mesoporous Silicon and Photocrosslinked Poly(Ester Anhydride)s. https://doi.org/10.13140/RG.2.1.1928.3923.

(11) Peppas, N. A.; Bures, P.; Leobandung, W.; Ichikawa, H. *Hydrogels in Pharmaceutical Formulations*. www.elsevier.com/locate/ejphabio.

(12) Brigham, N. C.; Ji, R. R.; Becker, M. L. Degradable Polymeric Vehicles for Postoperative Pain Management. *Nature Communications*. Nature Research December 1, 2021. https://doi.org/10.1038/s41467-021-21438-3.

(13) Ahmed, E. M. Hydrogel: Preparation, Characterization, and Applications: A Review. *Journal of Advanced Research*. Elsevier B.V. 2015, pp 105–121. https://doi.org/10.1016/j.jare.2013.07.006.

(14) Li, J.; Mooney, D. J. Designing Hydrogels for Controlled Drug Delivery. *Nature Reviews Materials*. Nature Publishing Group October 18, 2016. https://doi.org/10.1038/natrevmats.2016.71.

(15) Liaskoni, A.; Wildman, R. D.; Roberts, C. J. 3D Printed Polymeric Drug-Eluting Implants. *Int J Pharm* **2021**, *597*. https://doi.org/10.1016/j.ijpharm.2021.120330.

(16) Lemon, M. T.; Jones, M. S.; Stansbury, J. W. Hydrogen Bonding Interactions in Methacrylate Monomers and Polymers. *J Biomed Mater Res A* **2007**, *83* (3), 734–746. https://doi.org/10.1002/jbm.a.31448.

(17) Cristiani, T. R.; Filippidi, E.; Behrens, R. L.; Valentine, M. T.; Eisenbach, C. D. Tailoring the Toughness of Elastomers by Incorporating Ionic Cross-Linking. *Macromolecules* **2020**, *53* (10), 4099–4109. https://doi.org/10.1021/acs.macromol.0c00500.

(18) Chen, J.; Li, F.; Luo, Y.; Shi, Y.; Ma, X.; Zhang, M.; Boukhvalov, D. W.; Luo, Z. A Self-Healing Elastomer Based on an Intrinsic Non-Covalent Cross-Linking Mechanism. *J Mater Chem A Mater* **2019**, *7* (25), 15207–15214. https://doi.org/10.1039/c9ta03775f.

(19) Gu, S.; Skovgard, J.; Yan, Y. S. Engineering the van Der Waals Interaction in Cross-Linking-Free Hydroxide Exchange Membranes for Low Swelling and High Conductivity. *ChemSusChem* **2012**, *5* (5), 843–848. https://doi.org/10.1002/cssc.201200057.

(20) Groot, R. D.; Madden, T. J.; Tildesley, D. J. On the Role of Hydrodynamic Interactions in Block Copolymer Microphase Separation. *Journal of Chemical Physics* **1999**, *110* (19), 9739–9749. https://doi.org/10.1063/1.478939.

(21) Lim, K. S.; Galarraga, J. H.; Cui, X.; Lindberg, G. C. J.; Burdick, J. A.; Woodfield, T. B. F. Fundamentals and Applications of Photo-Cross-Linking in Bioprinting. *Chemical Reviews*. American Chemical Society October 14, 2020, pp 10662–10694. https://doi.org/10.1021/acs.chemrev.9b00812.

(22) Xie, H.; Yang, K. K.; Wang, Y. Z. Photo-Cross-Linking: A Powerful and Versatile Strategy to Develop Shape-Memory Polymers. *Progress in Polymer Science*. Elsevier Ltd August 1, 2019, pp 32–64. https://doi.org/10.1016/j.progpolymsci.2019.05.001.

(23) He, D.; Susanto, H.; Ulbricht, M. Photo-Irradiation for Preparation, Modification and Stimulation of Polymeric Membranes. *Progress in Polymer Science (Oxford)*. January 2009, pp 62–98. https://doi.org/10.1016/j.progpolymsci.2008.08.004.

(24) Akiba', M.; Hashim', A. S. *VULCANIZATION AND CROSSLINKING IN ELASTOMERS*; 1997; Vol. 22.

(25) Lin, X.; Zhao, X.; Xu, C.; Wang, L.; Xia, Y. Progress in the Mechanical Enhancement of Hydrogels: Fabrication Strategies and Underlying Mechanisms. *Journal of Polymer Science*. John Wiley and Sons Inc September 1, 2022, pp 2525–2542. https://doi.org/10.1002/pol.20220154.

(26) Molina, I.; Li, S.; Bueno Martinez, M.; Vert, M. *Protein Release from Physically Crosslinked Hydrogels of the PLA/PEO/PLA Triblock Copolymer-Type*; 2001; Vol. 22.

(27) Cervidil, P. *PRODUCT MONOGRAPH*; 1997.

(28) Akindoyo, J. O.; Beg, M. D. H.; Ghazali, S.; Islam, M. R.; Jeyaratnam, N.; Yuvaraj, A. R. Polyurethane Types, Synthesis and Applications-a Review. *RSC Advances*. Royal Society of Chemistry 2016, pp 114453–114482. https://doi.org/10.1039/c6ra14525f.

(29) Engels, H. W.; Pirkl, H. G.; Albers, R.; Albach, R. W.; Krause, J.; Hoffmann, A.; Casselmann, H.; Dormish, J. Polyurethanes: Versatile Materials and Sustainable Problem Solvers for Today's Challenges. *Angewandte Chemie - International Edition*. September 2, 2013, pp 9422–9441. https://doi.org/10.1002/anie.201302766.

(30) *ANNEX XVII TO REACH-Conditions of Restriction Restrictions on the Manufacture, Placing on the Market and Use of Certain Dangerous Substances, Mixtures and Articles*.

(31) Krone, C. A.; Klingner, T. D. Isocyanates, Polyurethane and Childhood Asthma. *Pediatric Allergy and Immunology*. August 2005, pp 368–379. https://doi.org/10.1111/j.1399-3038.2005.00295.x.

(32) Maisonneuve, L.; Lamarzelle, O.; Rix, E.; Grau, E.; Cramail, H. Isocyanate-Free Routes to Polyurethanes and Poly(Hydroxy Urethane)s. *Chemical Reviews*. American Chemical Society November 25, 2015, pp 12407–12439. https://doi.org/10.1021/acs.chemrev.5b00355.

(33) Bourguignon, M.; Thomassin, J. M.; Grignard, B.; Jerome, C.; Detrembleur, C. Fast and Facile One-Pot One-Step Preparation of Nonisocyanate Polyurethane Hydrogels in Water at Room Temperature. *ACS Sustain Chem Eng* **2019**, *7* (14), 12601–12610. https://doi.org/10.1021/acssuschemeng.9b02624.

(34) Nakibuule, F.; Nyanzi, S. A.; Oshchapovsky, I.; Wendt, O. F.; Tebandeke, E. Synthesis of Cyclic Carbonates from Epoxides and Carbon Dioxide Catalyzed by Talc and Other Phyllosilicates. *BMC Chem* **2020**, *14* (1). https://doi.org/10.1186/s13065-020-00713-2.

(35) Cornille, A.; Auvergne, R.; Figovsky, O.; Boutevin, B.; Caillol, S. A Perspective Approach to Sustainable Routes for Non-Isocyanate Polyurethanes. *European Polymer Journal*. Elsevier Ltd February 1, 2017, pp 535–552. https://doi.org/10.1016/j.eurpolymj.2016.11.027.

(36) Habets, T.; Siragusa, F.; Grignard, B.; Detrembleur, C. Advancing the Synthesis of Isocyanate-Free Poly(Oxazolidones)s: Scope and Limitations. *Macromolecules* **2020**, *53* (15), 6396–6408. https://doi.org/10.1021/acs.macromol.0c01231.

(37) Lamarzelle, O.; Durand, P. L.; Wirotius, A. L.; Chollet, G.; Grau, E.; Cramail, H. Activated Lipidic Cyclic Carbonates for Non-Isocyanate Polyurethane Synthesis. *Polym Chem* **2016**, *7* (7), 1439–1451. https://doi.org/10.1039/c5py01964h.

(38) Webster, D. C. Cyclic Carbonate Functional Polymers and Their Applications. *Prog Org Coat* **2003**, *47* (1), 77–86. https://doi.org/10.1016/S0300-9440(03)00074-2.

(39) Gennen, S.; Grignard, B.; Tassaing, T.; Jérôme, C.; Detrembleur, C. CO 2 -Sourced α-Alkylidene Cyclic Carbonates: A Step Forward in the Quest for Functional Regioregular Poly(Urethane)s and Poly(Carbonate)s . *Angewandte Chemie* **2017**, *129* (35), 10530–10534. https://doi.org/10.1002/ange.201704467.